5-2018

Effects of Surface-Directed Spinodal Decomposition on Binary Thin-Film Morphology

Michael Brian Wise
University of Arkansas, Fayetteville

Effects of Surface-Directed Spinodal Decomposition on Binary Thin-Film Morphology

A thesis submitted in partial fullfillment
of the requirements for the degree of
Master of Science in Mechanical Engineering

by

Michael Wise
University of Arkansas
Bachelors of Science in Mechanical Engineering, 2016

May 2018
University of Arkansas

This thesis is approved for recommendation to the Graduate Council.

Paul Millett, PhD
Thesis Director

Arun Nair, PhD
Committee Member

Min Zou, PhD
Committee Member

Abstract

Preferential wetting can have a significant impact on the kinetics of phase separation in certain systems. The depletion of the wetting component can simply alter domain growth rates or change the structure entirely. In this thesis, we employ a Cahn-Hilliard model to study the evolution of binary thin-films with symmetric surface wetting. Three possible morphologies were identified: discrete, bicontinuous, and a novel quasi-2D bicontinuous structure in which both phases retain continuity throughout the volume as well as on the center xy plane. Using a continuity factor, regions of film thickness versus blend composition were classified as producing a certain morphology. This region was then extended to further explore the possibilities offered by symmetric surface wetting. This information can guide future researchers to novel morphologies.

Acknowledgements

First and foremost, I would like to thank my advisor, Dr. Paul Millett, and the Millett Research Group for all of their help in both this project and the advancement of my knowledge of computer science. They have always been more than willing to discuss any issues I ran into and help find the best solution. Without them, none of this would have been possible. I would also like to thank the Arkansas Center for Advanced Surface Engineering for supporting this project, as well as the Arkansas High Performance Computing Center for providing the necessary resources and technical support.

Contents

Chapter 1

Introduction

1.1 Background

A number of interesting phenomena can occur as the thermodynamic properties of a system change. Most are familiar with the occurrences of freezing, melting and boiling. These shifts between states of matter are the most commonly known examples of phase transitions. However, a change of state is not required for a system to undergo phase transition. In actuality, a transition occurs anytime a break in the symmetry of a material is seen as the result of a change in its basic thermodynamic properties[1]. As in the above examples, this is normally brought about by a change in temperature, which will cause the formation or breaking of bonds as the system reaches a state of minimum free energy. This can result in a number of events. Changes of state are typically defined as first order transitions, so named due to the plateau of temperature that can be seen while energy is consumed or released to form the new state. This leads to a discontinuity in the first derivative of the system's energy. The remaining transformations have been classified as continuous transitions, which have a smooth variation in temperature, resulting in a smooth energy derivative. This type of transition was first conceived during studies of superconducting states in metals, but its real significance came with the idea of the order parameter [2]. The order parameter, commonly called a phase variable throughout this work, sprung from the idea that any continuous transition could be tracked by the evolution of a single variable across the material. Applying this concept to phase separation in alloys, Cahn and Hilliard developed a composition based equation to explain behaviors that were not characteristic of first order transitions [3]. Their model explained these formations using a free energy approximation to determine how local compositions would be affected. The new mode of separation which this described came to be known as spinodal decomposition, and it soon became one of the most popular topics in several fields of materials science.

Spinodal decomposition (SD) is a diffusion based un-mixing which was found to be

the cause of certain micro-structures in materials ranging from metals to fluid mixtures. The most common application of SD today is in the production of thin-film materials, which can have a range of thicknesses on both the nano and micro-scales. Given that thin-film technology has become a prominent feature in everything from electronics to filtration[4, 5], knowledge of their production processes has never been more important. It is crucial for some applications that a given internal structure is achieved, which has prompted decades of experimental and computational works on the topic. Through these experiments, several interesting mechanics that affect phase separation have been identified. One of the most pronounced effects is the preferential wetting of surfaces, often called surface-directed spinodal decomposition (SDSD). SDSD can play a significant role in determining film structure, as it results in a change of composition adjacent to the wetted surface. Indeed, it has been noted in experiments that domain evolution in these regions will follow much different trends than in the bulk of the blend [6–9]. Cases of both symmetric and single surface wetting have shown the potential for interesting morphologies [10–13]. However, the possibilities of utilizing SDSD for controlling structure remain largely unexplored.

Experimental studies of SDSD are generally limited to a few cases [6–8, 12, 13]. A small number of film thicknesses separated by hundreds of nanometers in thickness are used, and the majority are performed using evenly mixed blends [6, 7, 12, 14]. This is not surprising given the time necessary to produce and analyze these structures. In this aspect, computational modeling offers interesting opportunities. In recent years, the availability of computational resources has made simulation a valuable tool in materials science. Methods have been developed to model events at every length scale, including the range of sizes seen in SDSD. When concerned about the exact nature of the interactions that cause a behavior, molecular dynamics can be used. This method has been utilized several times to simulate small systems undergoing SDSD [15, 16] However, this can be too computationally intensive to model larger scales. Other methods have been developed that accurately portray the diffuse interfacial properties using a continuum approximation as opposed to particle based, lattice methods. Using the concept of the phase variable,

or order parameter, a system can be modeled using an approximation of the free energy to evolve the concentration at every location in a discretized space. This defines the phase field methods (PFM's), which have become a popular tool set in the study of meso-scale events, a group which includes the intermediate range of lengths seen in SD. Guided by experimental observations, PFM's have evolved from simple approximations to complex models that account for a variety of effects. Due to their efficiency and increased availability of computing power, these methods have been used not only to explain observed events, but to probe new areas at speeds that are difficult to match with experiment. This is not a new concept in phase separation studies. Several of the earliest experiments detailing SDSD cite computational works as their motivation to explore the topic [17]. Experiment and simulation in this area have developed a type of synergy that constantly pushes new limits.

In this spirit, we are using simulation to probe unexplored territory in the realm of symmetric surface wetting. It has been seen in experiment that a single material might be attracted to one or both of the external interfaces[12, 14]. But few works exist on the topic of symmetric wetting. As was previously mentioned, those that do are of a limited scope and leave much to be determined. This experiment will serve to clarify results found in previous studies while also extending our knowledge of SD mechanics in films sufficiently thin that the effects of preferential wetting can be seen throughout the film.

1.2 Objectives

The purpose of this thesis was to study the crossover of separation kinetics in thin-films with preferential surface wetting. The possibility of a transition from bulk separation to quasi-2D SD has been noted in experiments, but the conditions required are largely unexplored. For this reason, we have performed a parametric study in an effort to define the regions in which a selected morphology can be obtained. Initially, exploration of wetting effects on films of various thicknesses was performed to find where a crossover could be expected for our chosen concentrations. Once a reasonable space was defined, the likely morphology at each combination of film thickness and composition had to be determined. To achieve this goal, it was necessary to form an adequate definition of each

morphology that could be easily quantified. Using a continuity parameter, simulated systems of various thicknesses and compositions were classified by structure type. These regions were then extrapolated using simulations at conveniently spaced parameters for confirmation.

1.3 Organization

The remainder of this work is divided into five chapters. The next section, chapter two, will provide a thorough explanation of phase transitions in terms of the free energy of a system. Solution models will be derived from basic thermodynamic principles, chapter two will end with the initial explanations of continuous phase transitions. Chapter three is a survey of experimental and computational research relevant to the topics of general SD as well as SDSD in open and confined systems. Chapter four will describe the computational methods used for this experiment. This will include an explanation of common numerical methods, the specifics of our model, and the algorithms used for analyzing results. Chapter five will describe the findings of our experiment, including morphological classifications and discussion on how structures were formed. The final chapter will list what we were able to conclude given our findings and suggest future work in the area.

Bibliography

[1] Naoto Nagaosa. *Symmetry Breaking and Phase Transition*, pages 51–89. Springer Berlin Heidelberg, Berlin, Heidelberg, 1999.

[2] Navinder Singh. Thermodynamical phase transitions, the mean-field theories, and the renormalization (semi)group: A pedagogical introduction. 02 2014.

[3] John W. Cahn. Phase separation by spinodal decomposition in isotropic systems. *The Journal of Chemical Physics*, 42(1):93–99, 1965.

[4] Le Li, Xiaobo Shen, Sung Woo Hong, Ryan C. Hayward, and Thomas P. Russell. Fabrication of co-continuous nanostructured and porous polymer membranes: Spinodal decomposition of homopolymer and random copolymer blends. *Angewandte Chemie*, 124(17):4165–4170, 2012.

[5] Takahiro Ohe, Miki Kuribayashi, Ami Tsuboi, Kotaro Satori, Masao Itabashi, and Kazumasa Nomoto. Organic thin-film transistors with phase separation of polymer-blend small-molecule semiconductors: Dependence on molecular weight and types of polymer. *Applied Physics Express*, 2(12):121502, Nov 2009.

[6] P. Guenoun, D. Beysens, and M. Robert. Dynamics of wetting and phase separation. *Physical Review Letters*, 65(19):2406–2409, May 1990.

[7] Richard A. L. Jones, Laura J. Norton, Edward J. Kramer, Frank S. Bates, and Pierre Wiltzius. Surface-directed spinodal decomposition. *Physical Review Letters*, 66(23): 3087–3087, Oct 1991.

[8] Pierre Wiltzius and Andrew Cumming. Domain growth and wetting in polymer mixtures. *Physical Review Letters*, 66(23):3000–3003, Oct 1991.

[9] F. Bruder and R. Brenn. Spinodal decomposition in thin films of a polymer blend. *Physical Review Letters*, 69(4):624–627, 1992.

[10] Hajime Tanaka. Wetting dynamics in a confined symmetric binary mixture undergoing phase separation. *Physical Review Letters*, 70(18):2770–2773, Mar 1993.

[11] L. Sung, A. Karim, J. F. Douglas, and C. C. Han. Dimensional crossover in the phase separation kinetics of thin polymer blend films. *Physical Review Letters*, 76 (23):4368–4371, Mar 1996.

[12] Howard Wang and Russell J. Composto. Thin film polymer blends undergoing phase separation and wetting: Identification of early, intermediate, and late stages. *The Journal of Chemical Physics*, 113(22):10386–10397, Aug 2000.

[13] Hyun-Joong Chung and Russell J. Composto. Breakdown of dynamic scaling in thin film binary liquids undergoing phase separation. *Physical Review Letters*, 92(18), Jun 2004.

[14] M. Geoghegan, R. A. L. Jones, and A. S. Clough. Surface directed spinodal decomposition in a partially miscible polymer blend. *The Journal of Chemical Physics*, 103(7):2719–2724, 1995.

[15] S. Toxvaerd. Molecular dynamics simulations of spinodal decomposition in films of binary mixtures. *Physical Review Letters*, 83(25):5318–5321, 1999.

[16] Subir K. Das, Sanjay Puri, Jurgen Horbach, and K. Binder. Molecular dynamics study of phase separation kinetics in thin films. *Physical Review Letters*, 96(1), Dec 2006.

[17] R C Ball and R L H Essery. Spinodal decomposition and pattern formation near surfaces. *Journal of Physics: Condensed Matter*, 2(51):10303–10320, 1990.

Chapter 2

Scientific Background

2.1 Introduction

The science of phase transitions has seen several major advances in the last century. Since the development of early solutions theories, researchers have been working to both generalize descriptions to cover all materials, as well as fine-tune models to determine the exact interactions in a given mixture. In this section, the earliest relevant solution theories will be derived from the fundamental thermodynamics of a system. To build upon that work, one of the most important works in the study of phase transitions, the Landau theory of free energy, will be presented. Finally, the work leading up to and the conception of the Cahn-Hilliard model will be discussed.

2.2 Free Energy and Phase Separation

The states occurring in a binary mixture are determined by the fundamental thermodynamics of the blend at a given time. An isolated system will always tend towards a lower energy state, which could result in a phase transition or separation. The most common descriptor of a system's energy is the Gibbs Free Energy. Gibbs Free Energy, described as the maximum possible work that a system could perform at a constant pressure and temperature, is described by

$$G = H - TS \tag{2.1}$$

where H is the enthalpy of the system, T is its temperature, and S is its entropy. Enthalpy includes both the internal energy of the system, which can be determined through the inherent chemical bonding of that state, as well as the product of the system pressure and volume. The entropy is a measure of disorder in the system. To determine how these quantities will act at various compositions and temperatures, we expand this energy to describe the environment created by mixing. This is called the Gibbs Free Energy of Mixing, which is given by

$$\Delta G_{mix} = \Delta H_{mix} - T\Delta S_{mix} \tag{2.2}$$

where each term simply represents the change incurred when two components are mixed. Depending on the system, the free energy function could take on a variety of shapes, which would significantly affect the homogeneity of the mixture. One of three cases will occur. The first is the case of immiscibility, which is the result of a positive free energy with a negative second derivative. In this situation, mixing never occurs. The second case is that of total miscibility, which requires the free energy to be negative over the entire range with a positive curvature. This leads to a homogeneous mixture at all compositions and temperatures. The third, and most interesting case is that in which the free energy has several local minima, which leads to partial miscibility. Systems that fall into this category will have parametric regions of temperature and composition at which they will be mixed or have potential for separation. A typical temperature-composition phase diagram for this scenario can be seen in figure 2.1.

Several curves define the regions of miscibility as well as the stability of any structures that occur through transitions. The binodal, or the outer curve, is determined by the locations of the common tangent points on the free energy function. Under the binodal, phase separation is possible, but structures formed will only be stable against small fluctuations in composition. This metastable region encompasses the space between the binodal and the second curve, which is called the spinodal. The spinodal, which is outlined by the points of inflection of the free energy curve, encompasses a region of stable phase separation. It was previously thought that phase separation must take place after some form of nucleation. However, there is a fundamental difference between nucleation and growth and the mechanism that takes place in the spinodal region. By definition, the former requires the formation of a nucleus which will become stable at a certain size and the free energy profile will lead to growth through "downhill diffusion". The nature of this process requires that the system be located between the binodal and spinodal in order to both allow de-mixing and meet the need for upward concavity of free energy. Under the spinodal, mixtures can spontaneously separate through a rapid diffusion based de-

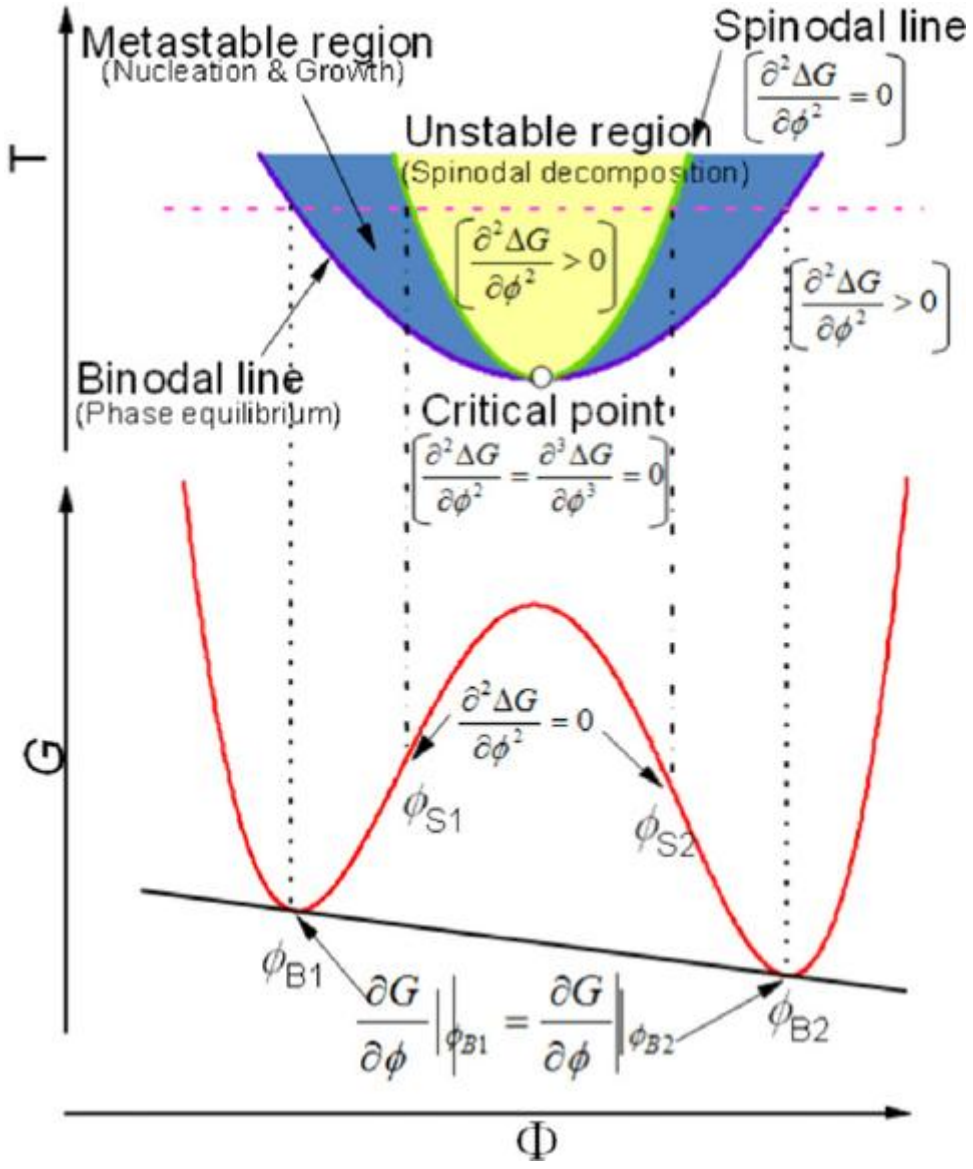

Figure 2.1: Phase diagram in relation to free energy curve of the system. The limits of the binodal and spinodal are denoted by ϕ_{B1}-ϕ_{B2} and ϕ_{S1}-ϕ_{S2} [1].

mixing due to the concavity of the energy profile. This led to vastly different structures, and has become a crucial mechanism in the production of several technologies [2–4]. The desire to explain these mechanisms in certain materials has brought about multiple phase transition theories, including several of the most widely used models in materials science.

2.3 Free Energy Solutions

Given that the free energy functional is the basis on which models of phase transitions are built, it is important that an accurate approximation is used. The components of free energy, as given by equation 2.2, are the enthalpy and entropy of mixing, which both

require the assumption of random mixing for standard mean-field approximations. The entropy of mixing is calculated by determining the number of configurations that the system can take. In order to determine the proper expression to describe configurations while mixing, it is necessary to begin by finding the isothermal entropy of expansion for an ideal gas. Beginning with the fundamental thermodynamic relation, we are given

$$dU = TdS - PdV \tag{2.3}$$

where P is the system pressure, and V is its volume[5]. Given the nature of an ideal gas, we can simplify this relation by assuming the differential internal energy is negligible and rearranging terms to the following form.

$$dS = \frac{PdV}{T} \tag{2.4}$$

Then, using the ideal gas equation, we can rewrite equation 4 as

$$\int_{S_2}^{S_1} dS = nR \int_{V_2}^{V_1} \frac{dV}{V} \tag{2.5}$$

where R is the ideal gas constant and n is the number of moles of gas[5]. Then considering the fact that the final volume will be the sum of the volumes of two mixed components (A and B), we can integrate for component A to obtain its change in energy[5].

$$\Delta S_A = nRln\Big(\frac{V_2}{V_1}\Big) = n_A Rln\Big(\frac{V_A + V_B}{V_A}\Big) \tag{2.6}$$

At this point, we can use the proportionality between the number of moles in an ideal gas and its volume to rewrite equation 6 using the mole fraction, χ_A,of the component[5]. This yields

$$\Delta S_A = -\chi_A Rln(\chi_A) \tag{2.7}$$

Using this form, it is possible to write the full molar entropy of mixing for a mixture of components A and B, as seen in equation 2.8.

$$\Delta S_{mix} = -R[\chi_A ln(\chi_A) + \chi_B ln(\chi_B)] \tag{2.8}$$

This can be further refined using the knowledge that the two fractions, χ_A and χ_B, have a sum of one. We are now able to express the entropy in terms of a single variable, χ_B[5].

$$\Delta S_{mix} = -R[(1-\chi_B) ln(1-\chi_B) + \chi_B ln(\chi_B)] \tag{2.9}$$

The second free energy component that we will need to consider, the enthalpy of mixing, will vary depending on the chosen model. The simplest is the ideal solution model, which assumes that a mixture will act similarly to an ideal gas. This would mean that all chemical bonds that occurred in both pure components and the mixture required similar amounts of energy to break and form, so no type of bond would be favored. This results in a negligible enthalpy of mixing, so the molar free energy of an ideal gas would be given by[5]

$$\Delta G_{mix,i} = RT[(1-\chi_B) ln(1-\chi_B) + \chi_B ln(\chi_B)] \tag{2.10}$$

However, few real mixtures act in this fashion. The change in internal energy that occurs when two species are mixed can rarely be ignored, which raised the need for an alternative. This came about with the development of the regular solution model. It was based in the theory of a randomly mixed composition throughout with molecules having an average coordination number, z[5]. If there are n_A particles of A, they will form roughly $z \times n_A$ bonds. Given the molar fraction of B, χ_B, we can say that some portion of those bonds, roughly $\chi_B \times n_A$, will connect A and B molecules[5]. This allows us to define the difference in internal energy incurred by mixing B into pure A and A mixing into pure B as

$$\Delta U_{mix,A} = \chi_B z n_A (\epsilon_{AB} - \epsilon_{AA}) \tag{2.11}$$

$$\Delta U_{mix,B} = \chi_A z n_B (\epsilon_{AB} - \epsilon_{BB}) \tag{2.12}$$

where ϵ_{AB}, ϵ_{AA} and ϵ_{BB} are the bond energies between molecules of A and B, pure A, and pure B, respectively[5]. The total internal energy change of mixing can be given by the sum of these terms, with a coefficient of one-half to prevent double-counting of bonds

$$\Delta U_{mix} = \frac{1}{2}[\chi_A z n_B (\epsilon_{AB} - \epsilon_{BB}) + \chi_B z n_A (\epsilon_{AB} - \epsilon_{AA})] \tag{2.13}$$

By expanding the coefficients using the definitions of the molar fractions and combining like terms, we can reach the most commonly used definition for the enthalpy of mixing,

$$\Delta U_{mix} = \frac{z}{2}\chi_A \chi_B (2\epsilon_{AB} - \epsilon_{AA} - \epsilon_{BB}) = \beta(1 - \chi_B)\chi_B \tag{2.14}$$

where β is called the interaction parameter, and serves to lump energy related terms into a single coefficient for simplicity[5]. This allows for the expression of free energy using the regular solution model through one variable, χ_B, as seen below.

$$\Delta G_{mix} = \beta(1 - \chi_B)\chi_B + RT[(1 - \chi_B)ln(1 - \chi_B) + \chi_B ln(\chi_B)] \tag{2.15}$$

These standard mean field approximations formed the basis which further solution theories were built on past the early 1900's[6]. In the field of phase transitions, one of the largest contributions was due to Lev Landau in 1937 [7]. During his studies, he noticed a unifying concept among several transitions. A series of phenomena could be described in terms of broken symmetry in a field of some conserved value, later called the order parameter. In his theory, when a system was in its random, or symmetrical phase, the relevant order parameter would be zero, while more ordered structures would result in a non-zero value. This led Landau to describe continuous, or second order, phase transitions as a series expansion around the order parameter, Ψ, for a given situation. Based on the fact that energy the difference should be non-zero values and not their signs, terms with odd powers were ignored [7]. This gave the fundamental Landau theory

$$G = \frac{1}{2}\alpha(T)\Psi^2 + \frac{1}{4}\gamma(T)\Psi^4 + ... \tag{2.16}$$

where α and γ are both temperature based coefficients, which are commonly assigned a value of one for simplicity. This simplified version of bulk free energy has become the basis of numerous theories and models. These include several variations of equation 2.16, including the Ginzburg-Landau free energy, which adds a term to consider critical mixtures, and Landau-de Gennes theory, which integrates Landau theory into another Mean-Field approximation called the Flory-Huggins model.

2.4 Spinodal Decomposition

Early evidence of non-nucleation phase separation events was discovered during studies of the compositions of alloys. The first notable experiments that gave evidence of this mechanism were studies of X-ray diffraction patterns in Cu-Ni-Fe alloys [8]. This prompted further analysis by Daniel and Lipson who concluded that the compositional changes were periodic with an alloy specific wavelength [8]. This group gave no exact conclusion on the reason behind these fluctuations, but they did believe that the periodic structure could be the beginning of standard phase separation. It was later theorized that the observed compositions could not have been the result of nucleation and growth, so an alternative type of separation must exist. Given the knowledge that negative diffusivity could occur in the spinodal region [9], several researchers attempted to explain the model through Fick's laws of diffusion. However, these were unable to capture the modulations described by previous experiments. The first successful attempt to model the diffusive nature of these systems was given by Mats Hillert. In his doctoral thesis, Hillert formulated a model which used the regular solution for the free energy of mixing to define the interaction between the species on a lattice. This one-dimensional model almost undoubtedly proved the significance of the spinodal region to stability in phase separation by showing fluctuations similar to those seen in previous experiments. However, it was found to be incomplete due to its inability to account for interfacial regions, which is a problem inherent to coarse-grained, lattice methods. Building on the work of Hillert, John W. Cahn and John E. Hilliard made one of the most significant contributions to this

field to date. In their collaborative work, they determined that the interaction should not only include the free energy of the uniform solution, but also the effects of the difference in composition over a region [9]. The general Cahn-Hilliard equation is given by

$$\frac{\partial \phi}{\partial t} = \nabla \cdot \left(M \nabla \frac{\delta F}{\delta \phi} \right) \tag{2.17}$$

where ϕ represents the system composition, M is the mobility, and F is the free energy functional to describe the system. The free energy could be expanded into the form of equation 2.18

$$F = \int [f_0 + \kappa (\nabla \phi)^2] dV \tag{2.18}$$

where f_0 is the free energy of a homogeneous blend of composition ϕ and the gradient term serves to emulate the effects of interfacial regions. The gradient term penalizes excessive boundaries between regions, which leads to a more realistic structure after coarsening. The bulk free energy can take several forms, the most common of which is the Ginzburg-Landau energy. However, a series of functionals based in Flory-Huggins theory and alternative solutions derived from Landau theory have been shown to model specific types of systems with good qualitative accuracy. The Cahn-Hilliard equation grew to be one of the most widely used methods of modeling phase separation, particularly spinodal decomposition, in a range of materials. After its acceptance as the primary model for phase separation in alloys, it was also applied to a variety of liquid mixtures, including polymer blends, petrochemicals, and alcohols [10, 11]. Its wide range of uses led to expansions of the model, which included the addition of random thermal fluctuations, microfluidics, and interactions for specific polymer blend. The Cahn-Hilliard-Cook model became the new standard due to the reality of random thermal noise in experiment, and it will be discussed at greater length in later chapters.

Bibliography

[1] Yuki Ochi, Rie Kawakubo, Dan-Thuy Van-Pham, Yuki Kitamura, Hideyuki Nakanishi, Tomohisa Norisuye, and Qui Tran-Cong-Miyata. Phase separation of polymer mixtures induced by light and heat: A comparative study by light scattering. 6:

045002, 10 2015.

[2] Le Li, Xiaobo Shen, Sung Woo Hong, Ryan C. Hayward, and Thomas P. Russell. Fabrication of co-continuous nanostructured and porous polymer membranes: Spinodal decomposition of homopolymer and random copolymer blends. *Angewandte Chemie*, 124(17):4165–4170, 2012.

[3] Takahiro Ohe, Miki Kuribayashi, Ami Tsuboi, Kotaro Satori, Masao Itabashi, and Kazumasa Nomoto. Organic thin-film transistors with phase separation of polymer-blend small-molecule semiconductors: Dependence on molecular weight and types of polymer. *Applied Physics Express*, 2(12):121502, Nov 2009.

[4] Seung-Won Song and John M. Torkelson. Coarsening effects on microstructure formation in isopycnic polymer solutions and membranes produced via thermally induced phase separation. *Macromolecules*, 27(22):6389–6397, 1994.

[5] The thermodynamics of regular and ideal solutions.

[6] J. H. Hildebrand. A history of solution theory. *Annual Review of Physical Chemistry*, 32(1):1–24, 1981.

[7] Valery Pokrovsky. Landau and theory of phase transitions. 03 2009.

[8] Vera Daniel and H Lipson. An x-ray study of the dissociation of an alloy of copper, iron and nickel. 181:368–378, 01 1943.

[9] John W. Cahn. Phase separation by spinodal decomposition in isotropic systems. *The Journal of Chemical Physics*, 42(1):93–99, 1965.

[10] P. Guenoun, D. Beysens, and M. Robert. Dynamics of wetting and phase separation. *Physical Review Letters*, 65(19):2406–2409, May 1990.

[11] Richard A. L. Jones, Laura J. Norton, Edward J. Kramer, Frank S. Bates, and Pierre Wiltzius. Surface-directed spinodal decomposition. *Physical Review Letters*, 66(23): 3087–3087, Oct 1991.

Chapter 3

Literature Review

3.1 Introduction

The phenomena of spinodal decomposition and surface-directed spinodal decomposition have been observed by many experimentalists and modelers. This chapter will begin with a brief review of several materials in which spinodal decomposition was observed, as well as the initial models and laws used to describe their late stage morphologies. This will be followed by a description of the mechanism of surface-directed spinodal decomposition and a review of research focused on the interplay between surface effects and bulk separation. In the last section, the situation of thin-films with symmetric surface wetting will be discussed, including the observed stages of evolution and techniques used to model these systems.

3.2 Spinodal Decomposition

After the work of Cahn and Hilliard, a plethora of theories were developed both to increase its qualitative accuracy and to better describe transitions in other materials. One of the first modified Cahn-Hilliard theories was presented by H. E. Cook, and has come to be known as the Cahn-Hilliard-Cook equation [1]. The basic model assumed that a system coarsened without thermal fluctuations, which caused the model to diverge from realistic behavior with time. Cook suggested the addition of a stochastic term, specifically a random white noise, which could account for potential variance due to thermal effects. This began a series of attempts to rectify the late stage growth dynamics of systems in the spinodal region with traditional models. At this point, it was somewhat well accepted that after initial spinodal decomposition and development of discrete domains, the time scale of growth changed. The most commonly accepted theory was that of Lifshitz and Slyozov, who said that the growth of domains proceeded through Ostwald ripening [2]. This resulted in discrete domains diffusing through another phase in order to coalesce and form larger clusters while maintaining overall self-similarity. Several numerical studies were performed in order to provide a more fundamental description of this mechanism.

The first of these was due to Binder and Stauffer in 1974 [3]. The group described these events from the scale of individual molecules breaking from and reconnecting to a cluster. They determined that, below a temperature and composition dependent cluster size, the tendency of molecules to diffuse towards a higher concentration would cause the center of the smaller cluster to shift. This eventually led to the coalescence of this cluster with a nearby domain, which would reduce the amount of phase interface and lower the free energy of the system. Other temperature domains saw a slower mechanism, which was determined to be diffusion of individual molecules over short distances between clusters. This theory as well as a coarse grained model proposed by Langer et al [4] were both tested through simulation and experiment. Both showed good agreement with recent Monte-Carlo simulations, but the theory of Binder and Stauffer was proven accurate over a greater range of times [2]. Nojima and Tsutsumi came to similar conclusions in their studies of small molecule polymer blends [5]. The results were somewhat consistent with the theory of Langer et al, but the obtained power law fit was in better agreement with Binder and Stauffer [3]. Both of these theories were considered in later studies by Eric Siggia, who focused on extending the time period over which coarsening dynamics could be predicted in liquids[2]. Siggia's theory divided growth into regimes based on composition and the resulting domain density after the initial decomposition. In early time, they agreed that the separation could be modeled using the Cahn-Hilliard-Cook equation. However, as the system coarsens into discrete domains, the mechanisms described in previous theories become dominant. A combination of Ostwald ripening and coalescence of domains results in an altered growth rate throughout late stages. However, the difference in density of the two components can also come into play, leading to a second increase in the rate of coarsening. This theory was partially confirmed for a series of polymer blends by Hashimoto et al [6]. However, certain dynamics of polymer mixing could not be described accurately using a traditional Cahn-Hilliard-Cook methods. Nojima et al found that in mixtures of polystyrene and poly(methylphenylsiloxane) a reasonable approximation could not be reached using linearized Cahn-Hilliard-Cook theory [5]. The traditional Ginzburg-Landau free energy functional was found to be inadequate for polymers above

a certain chain length. The effects of reptation for long polymers cause diffusion mechanics that are more difficult to predict than those of small molecules. This was partially addressed by the development of the Flory-Huggins free energy functional for polymer mixtures, which is given by

$$\Delta G_{mix} = kT \left[\frac{1-\phi_B}{N_A} ln(1-\phi_B) + \frac{\phi_B}{N_B} ln(\phi_B) + \chi \phi_B (1-\phi_B) \right] \tag{3.1}$$

where N_A is the degree of polymerization of component A, N_B is the degree of polymerization of component B, and χ is an interaction parameter describing the specific blend, which will often favor segregation [7, 8]. The Flory-Huggins free energy was initially developed to describe the interactions that occured when a polymer was dissolved in a solvent. However, it was quickly adapted to fit polymer blends, which became an area of significant interest in the mid-1970's. The Flory-Huggins energy was adapted by de Gennes and Pincus in 1980 and 1981, respectively, to consider alterations of the gradient term which would more accurately represent interfacial effects in binary polymer blends. This model was immediately recognized, tested and expanded upon. As early as 1983, Binder used the de Gennes extension to Flory-Huggins theory to develop a Cahn-Hilliard style model for general phase separation in polymer blends[9]. The theory was also confirmed through several experiments throughout the following decade. Hashimoto et al found this model to accurately describe behavior over several time regimes in mixtures of styrene-butadiene and polybutadiene [6]. The same group later discovered some dissonance when comparing coarsening kinetics of long-chain polymer mixtures to the previously existing theories [10]. However, they did attribute the differences to entanglement of the chains as had been predicted by de Gennes and earlier theories [7]. Despite the potential for increased accuracy, the Flory-Huggins-de Gennes free energy was not commonly used in modeling. The difficulty of deriving appropriate expressions for mobility to describe real systems was not often justified when slight modification to a standard Ginzburg-Landau energy would likely suffice.

3.3 Surface-Directed Spinodal Decomposition

As studies of spinodal decomposition became more common, a new effect was noticed throughout several experiments. The kinetics of phase separation often changed near the outer boundaries of the mixture, which were in contact with either open air or a substrate. The interface between the mixture and its surrounding often saw a large concentration of one material, which would then change the internal structure. The earliest studies of this property were due to Guenoun et al in 1989 [11]. In mixtures of methanol and cyclohexane, they noticed a high concentration of methanol near both the air and the quartz substrate on which the experiment was conducted. They showed that both surfaces were completely wetted by methanol, and that layer remained connected to the same phase in the bulk. As a result, the region adjacent to the wetting layer saw the formation and coalescence of cyclohexane domains which showed markedly different growth than expected for bulk material[11]. However, as the system coarsened, flow of methanol from the bulk fed the increasing thickness of the wetting layer until the capillaries connecting the two were consumed. The result was a methanol layer surrounding a matrix of the cyclohexane that contained small droplets of methanol. The growth laws were not easily determined, and the group was not certain what led to the formation of the wetting layer. There were several theories on what caused the formation of wetting layers. One of the first models to achieve similar behavior was that of Ball and Essery in 1990 [12]. Theirs was essentially a study of boundary conditions prompted by the temperature quenches used in experimental studies. Ball and Essery made the point that, despite the low thickness of the films being studied, a temperature quench was not truly instantaneous. The group developed a finite difference method to solve the Cahn-Hilliard-Cook model with coefficients that vary as the result of a typical temperature diffusion equation. Using their model, they showed the structures that would be obtained as a system coarsens due to various types of quenches. Starting with an instantaneous quench, the model showed typical spinodal decomposition. However, when the simulated cooling front moved slowly across the material, a layered structure was observed. The results of interest for surface effects were obtained with a median quench rate, which resulted in a layered

structure near the simulated heat sink and a typical bicontinuous network at greater depth. While these were similar to the desired structures, it was later found that these were simply the results of the off-critical nature of the simulated system. Further theories on the nature of the wetting layer were formulated during the following years. The first work to use the term "surface-directed spinodal decomposition" offered an alternative explanation which focused on both broken symmetry and preferential attraction between one material and the air or substrate[13]. Jones et al experimented with a mixture of poly (ethylene propylene) (PEP) and its perdeuterated form (dPEP). The group witnessed the formation of a d-PEP layer at the outer surfaces and corresponding changes in nearby separation kinetics. However, they did not believe quench speed was the culprit. It was hypothesized that the shorter and less polarizable deuterium bonds led to a lower surface energy, and thus, the segregation of d-PEP to the outer interfaces. This theory was built upon by Wiltzius and Cumming in their studies of polymer mixture [14]. They reported similar behavior, and they were the first to attribute the preferential attraction of the substrate to long-range van der Waals forces. By this point, the explanation of preferential attraction was widely accepted. Moving forward, computational studies used altered energy profiles to model the attraction and ensure realistic surface wetting. The first of these simulations was the work of Brown and Chakrabarti [15], who used a two-dimensional Cahn-Hilliard-Cook model. In order to ensure wetting, the group forced two conditions. The first was that the surface to be wetted was set to keep the order parameter at the value of the preferred phase. The second, which guaranteed growth, altered the surface energy as a function of distance from the preferred surface. Coupled with the ability to vary quench depth through further alterations of the Ginzburg-Landau free energy, this model became a powerful tool for probing the possibilities of thin-film systems. Starting with a strong surface attraction, which mimics a long-range van der Waals force, they achieved growth of the wetting layer which matched the diffusion limited theories of Lifshitz and Slyozov [16] across both quench depths. For the short range potential, they saw separation that followed typical theories of spinodal decomposition. The results obtained were in agreement the experimental work of Jones et al regarding the

strength of the preferential attraction. Domains growth was seen to occur at a similar rate both parallel and perpendicular to the free surface. In wetting cases, the length scales were also seen to be larger in planes parallel to the layer, which was in agreement with previous works [11, 13]. Growth rates found to be inconsistent with experiments were attributed to the model's lack of an appropriate hydrodynamic scheme, and several models confirmed these results. Both an analysis by through molecular dynamics and a later simulation study by Chen and Chakrabarti confirmed that hydrodynamic pumping would result in a faster wetting layer growth rate [17]. However, as computational studies continued, several models based on that of Brown were able to confirm that similar results would be obtained at the surface and in nearby regions with or without fluid effects [18, 19]. All of these experiments and many others shared one aspect. They focused on the case of one material wetting a single surface. There are many situations in which this will not be the case. Experiments by Bruder and Brenn pointed to the potential for interesting structures when wetting comes into play on both the top and bottom of a film [20]. In their case, the air interface was totally wetted by one polymer while columnar structures likely protruded from that layer to the opposite interface. Although the substrate in this experiment showed no preferential wetting, it did prove that alternative structures could be achieved through a combination of surface effects and low film-thickness. Further studies involving variation of film thickness with surface wetting were performed by Geoghegan et al [21]. The results of this experiment largely resembled those obtained in previous works on polymer blends [13, 14]. However, one of their films, which was determined to be below a threshold of 1.5 times the spinodal wavelength of the blend, showed different dynamics. This prompted a similar study by Sung et al focused on the differences seen as film-thickness reached and passed this crossover [22]. Using a similar polymer blend, they prepared films slightly above and far below the spinodal wavelength of the mixture. Upon quenching, the higher thickness film showed variations in composition that indicated SDSD with typical bulk kinetics in the central region of the film. Films of lower thickness showed something much more similar to two-dimensional separation. While the causes and implications of these results

were not clear, they did offer some view of the morphologies that were attainable due to the formation of wetting layers in thin-film blends. Moving forwards, researchers placed increasing interest not only on the effects of film thickness, but also on new materials and experimental arrangements that could provide more information on the nature of surface wetting.

3.4 Symmetric Surface-Directed Spinodal Decomposition

Even before the works of Geoghegan and Sung, researchers had begun to study the effects that film thickness could have on morphology. The work of Tanaka et al studied these from a different perspective by altering the surfaces confining the mixture [23]. Using a small diameter tube and two parallel plates of the same material, which they called one and two-dimensional capillaries, the group studied how systems would react if the surrounding environment was composed of a single material. In the one-dimensional case, they saw surface wetting of the entire capillary, with columns of a limited diameter connecting opposite sides. The columns formed remained stable through later stages in both liquid and polymer mixtures. However, a different coarsening process was noted in the two-dimensional tests. Like the first case, initial stages involve the formation of wetting layers and a bicontinuous network in the central region. At later times, the lack of geometrical constraints on the tubes that bridge the wetting layers come into play. While the layers do grow due to flow of wetting material from the central region, they do not stabilize as was seen in the one-dimensional capillary. Instead, the layers reach a thickness that seemed to result in backflow to the columns. Eventually the wetting layers were consumed by the columns and they became disk-shaped domains. Further compositional studies continued to explore the region without giving exact descriptions of the morphological evolutions that occurred. Wendlandt et al [24] presented composition profiles of polymer blends with various "boundary conditions" that would closely match modeling experiments by Binder [18]. Their results both agreed with the general trends of experiments that utilized asymmetric boundary conditions, and studied the effects of quench depth on evolution of symmetrically bound mixtures. Using the model of Binder [18], they predicted two morphologies for the ranges of temperatures separated by

the "wetting transition temperature" in the same blend. The first resulted in a partial wetting scenario, where domains of both materials were in contact with the surfaces and a fairly even composition would be seen through out. However, the case above the wetting transition temperature was markedly different. Wetting layers were predicted at both surfaces, which resulted in columnar domains connecting the two. This scenario, which seemed to minimize the free energy for un-mixing systems of this type, offered one explanation of the compositions the group obtained. They noted a lack of the second material near each of the confining surfaces, with a nearly even ($\approx$55% non-wetting) composition throughout the central region. With the proper film thickness, this would have likely corresponded to the predicted structure. It was proposed that a more realistic morphology, as a result of both composition and annealing time, would be a suspension of wetting material droplets in a non-wetting material matrix. That results in a nearly even composition, which matched their findings. This was probable, but the group could not confirm what structures were formed. Work in this field was continued by Wang and Composto, who more accurately characterized the stages of evolution under symmetric wetting conditions [25]. They used a blend in which one component wetted both the air and the substrate to achieve similar wetting layers at both extremes. In the early stages, they saw initial segregation of the deuterated poly(methyl methacrylate) (dPMMA) to the top and bottom while the central region displayed a bicontinuous structure typical of spinodal decomposition. Due to pumping of the wetting phase from the bulk, this stage is also characterized by a higher surface roughnness as pressure from the capillaries forces an uneven distribution. The flow of the preferred material was reversed in the intermediate stage when the layer has reached its peak thickness. This phase occurs when the inner layer has separated into a largely columnar structure. These columns grow due to back-flow from the wetting layers, which results in lower thickness and surface roughness for the layer formed at the free surface. Eventually, the domains in the central region will rupture to form a bicontinuous network. Portions of this network will then coalesce, leading to large droplets of the non-wetting material covered by the wetting layers. During the documentation of these stages, the exact mechanism that

caused them was not well understood. Further research by Chung and Composto helped to elucidate the relationship between symmetric wetting and bulk separation dynamics [26]. Using PMMA and poly(styrene-ran-acrylonitrile) (SAN), the group explored the effects of film thickness and composition on late stage morphology. In films that were roughly 700nm thick, the expected morphology of discrete droplets was observed in a 50:50(PMMA:SAN) blend. However, as the composition of the film was varied, the effects of the wetting layers became more apparent. Significant differences were noted in the evolution of 70:30 blends. The 2D bicontinuous structure, typical of early stages, remained and coarsened into a similar form at a larger scale. They continued by exploring several thicknesses over a wide range. They found that the confinement imposed by the symmetric wetting conditions caused slower domain growth as film thickness decreased. Their proposed explanation was that pumping of the materials was impeded by the low film thickness. No exact relation for bicontinuous growth was determined. The works of Chung, Wang, and Composto were of immediate interest to the modeling community. Das and coworkers published a work detailing their simulation of symmetric systems with both partial and complete wetting only a year later[27]. The group used a 3D PFM with a free energy modified near the surfaces to control surface attraction. Their results for the case of partial wetting showed the formation of disc-like domains, similar to those described in previous experiments. Their simulations of the complete wetting case yielded similar results for late stages, but they showed columnar domains similar to those described by Wang and Composto in early times [25]. The same group published a second computational experiment utilizing a molecular dynamics simulation as opposed to the conventional PFM. This model, based on a modified Lennard-Jones potential, was able to produce structures that were qualitatively similar to their continuum model. However, the computational expense of molecular dynamics meant they had to limit both the size and time of their simulations. This yielded only enough information to confirm its accuracy for very early stages of SDSD. In a later work, Puri, who collaborated with Das for the previous two articles, further studied SDSD with complete, symmetric wetting. Using a similar molecular dynamics simulation to that of Das[28], Puri showed that the

kinetics of SDSD are relatively unaffected by an increase in surface attraction past the point of complete wetting. Building on this work, Naraigh and Thiffeault developed a Navier-Stokes/CH model in an attempt to explain the events leading to rupture in late stage coarsening [29]. While the model did demonstrate some qualitative information, it was limited by unrealistic boundary conditions that did not properly describe the free surface. It was not until new methods were applied by a separate group that a sufficient explanation of late stage coarsening was offered. Hore and Laradji designed a dissipative particle dynamics model that went beyond the small size and times previously studied by Das and coworkers [30]. The group was able to replicate the early, intermediate, and late stages as defined by Wang and Composto. More importantly, their results provided a clear view of these stages and their transitions, which would be difficult to obtain experimentally. The shift from the initial to intermediate stage as well as the intermediate to late stage were found to be related to the average domain size. In the latter case, the this refers to the widths of the columns connecting the wetting layers. As the relevant domain length scale approaches the thickness of the film, separation kinetics are altered due to interaction between the domains. This causes growth of domains above the film thickness, which eventually leads to the late stage rupture described by Wang and Composto [25].

Bibliography

[1] J. Marro and J.l. Valles. Relevance of the cahn-hilliard-cook theory at early times in spinodal decomposition. *Physics Letters A*, 95(8):443–446, 1983.

[2] Eric D. Siggia. Late stages of spinodal decomposition in binary mixtures. *Physical Review A*, 20(2):595–605, Jan 1979.

[3] K. Binder and D. Stauffer. Theory for the slowing down of the relaxation and spinodal decomposition of binary mixtures. *Physical Review Letters*, 33(17):1006–1009, 1974.

[4] J. S. Langer, M. Bar-On, and Harold D. Miller. New computational method in the theory of spinodal decomposition. *Physical Review A*, 11(4):1417–1429, Jan 1975.

[5] Shuichi Nojima, Katsuaki Tsutsumi, and Takuhei Nose. Phase separation process in polymer systems. i. light scattering studies on a polystyrene and poly(methylphenylsiloxane) mixture. *Polymer Journal*, 14(3):225–232, 1982.

[6] Tatsuo Izumitani and Takeji Hashimoto. Slow spinodal decomposition in binary liquid mixtures of polymers. *The Journal of Chemical Physics*, 83(7):3694–3701, 1985.

[7] PG De Gennes. Dynamics of fluctuations and spinodal decomposition in polymer blends. *The Journal of Chemical Physics*, 72(9):4756–4763, 1980.

[8] P Pincus. Dynamics of fluctuations and spinodal decomposition in polymer blends. ii. *The Journal of Chemical Physics*, 75(4):1996–2000, 1981.

[9] K. Binder. Collective diffusion, nucleation, and spinodal decomposition in polymer mixtures. *The Journal of Chemical Physics*, 79(12):6387–6409, 1983.

[10] Takeji Hashimoto, Masahiko Itakura, and Hirokazu Hasegawa. Late stage spinodal decomposition of a binary polymer mixture. i. critical test of dynamical scaling on scattering function. *The Journal of Chemical Physics*, 85(10):6118–6128, 1986.

[11] P. Guenoun, D. Beysens, and M. Robert. Dynamics of wetting and phase separation. *Physical Review Letters*, 65(19):2406–2409, May 1990.

[12] R C Ball and R L H Essery. Spinodal decomposition and pattern formation near surfaces. *Journal of Physics: Condensed Matter*, 2(51):10303–10320, 1990.

[13] Richard A. L. Jones, Laura J. Norton, Edward J. Kramer, Frank S. Bates, and Pierre Wiltzius. Surface-directed spinodal decomposition. *Physical Review Letters*, 66(23): 3087–3087, Oct 1991.

[14] Pierre Wiltzius and Andrew Cumming. Domain growth and wetting in polymer mixtures. *Physical Review Letters*, 66(23):3000–3003, Oct 1991.

[15] Gregory Brown and Amitabha Chakrabarti. Surface-directed spinodal decomposition in a two-dimensional model. *Physical Review A*, 46(8):4829–4835, Jan 1992.

[16] I.m. Lifshitz and V.v. Slyozov. The kinetics of precipitation from supersaturated solid solutions. *Journal of Physics and Chemistry of Solids*, 19(1-2):35–50, 1961.

[17] Hao Chen and Amitabha Chakrabarti. Hydrodynamic effects on domain growth in off-critical polymer blends. *The Journal of Chemical Physics*, 108(14):6006–6013, Aug 1998.

[18] Kurt Binder, Sanjay Puri, and Harry L. Frisch. Surface-directed spinodal decomposition versus wetting phenomena: Computer simulations. *Faraday Discussions*, 112: 103–117, 1999.

[19] Sorin Bastea, Sanjay Puri, and Joel L. Lebowitz. Surface-directed spinodal decomposition in binary fluid mixtures. *Physical Review E*, 63(4), 2001.

[20] F. Bruder and R. Brenn. Spinodal decomposition in thin films of a polymer blend. *Physical Review Letters*, 69(4):624–627, 1992.

[21] M. Geoghegan, R. A. L. Jones, and A. S. Clough. Surface directed spinodal decom-

position in a partially miscible polymer blend. *The Journal of Chemical Physics*, 103(7):2719–2724, 1995.

[22] L. Sung, A. Karim, J. F. Douglas, and C. C. Han. Dimensional crossover in the phase separation kinetics of thin polymer blend films. *Physical Review Letters*, 76 (23):4368–4371, Mar 1996.

[23] Hajime Tanaka. Wetting dynamics in a confined symmetric binary mixture undergoing phase separation. *Physical Review Letters*, 70(18):2770–2773, Mar 1993.

[24] Michael Wendlandt, Tobias Kerle, Marcus Heuberger, and Jacob Klein. Phase separation in thin films of polymer blends: The influence of symmetric boundary conditions. *Journal of Polymer Science Part B: Polymer Physics*, 38(6):831–837, 2000.

[25] Howard Wang and Russell J. Composto. Thin film polymer blends undergoing phase separation and wetting: Identification of early, intermediate, and late stages. *The Journal of Chemical Physics*, 113(22):10386–10397, Aug 2000.

[26] Hyun-Joong Chung and Russell J. Composto. Breakdown of dynamic scaling in thin film binary liquids undergoing phase separation. *Physical Review Letters*, 92(18), Jun 2004.

[27] Subir K. Das, Sanjay Puri, Jurgen Horbach, and K. Binder. Kinetics of phase separation in thin films: Simulations for the diffusive case. *Physical Review E*, 72 (6), 2005.

[28] Sanjay Puri. Interplay of wetting and phase separation at surfaces. *Physica A: Statistical Mechanics and its Applications*, 384(1):100–107, 2007.

[29] Lennon O Naraigh and Jean-Luc Thiffeault. Dynamical effects and phase separation in cooled binary fluid films. *Physical Review E*, 76(3), 2007.

[30] Michael J. A. Hore and Mohamed Laradji. Dissipative particle dynamics simulation of the interplay between spinodal decomposition and wetting in thin film binary fluids. *The Journal of Chemical Physics*, 132(2):024908, 2010.

Chapter 4

Methods

4.1 Introduction

Landau's use of a single order parameter, sometimes called the phase variable, greatly reduced the complexity of describing continuous phase transitions. Over the course of several decades, a series of similar methods were developed to more accurately model systems of interest. With the formulations of the CH equation and its derivatives [1], researchers were able to accurately describe the kinetics of phase separation in a series of mixtures. Using these models, it became possible to obtain the compositional trends that occur in a mixture. However, due to the inherent difficulty of solving large sets of equations, these methods did not reach their full potential until significant advances were made in the field of computing. With increased access to computing resources, the field of simulation has exploded since the 1980's, bringing us into the modern era of research. Soon after these resources became available for research, simulation techniques were developed so that a more detailed understanding of continuous transitions could be attained. These have come to be known as the phase-field methods, which encompass all techniques that describe a situation through updating an array that stores the phase variable. A phase-field method discretizes the evolution in both time and space, and updates are performed at a given time interval based on values of the order parameter previously stored near that location. The following section will describe the common computational approaches used to solve the Cahn-Hilliard equation, which is the most common governing equation for this family of methods. An explanation of both finite-difference and fourier based approximations will be provided, along with an explanation of the boundary conditions used. The algorithm used for processing of results will also be described, and our criterion for determining morphology of a structure will be discussed.

4.2 Finite Difference vs Fourier Methods

As has been demonstrated in literature [2–4], it is possible to model many types of systems in both two and three dimensions using phase field methods. For our purposes,

it was necessary to understand the simulation of an immiscible binary fluid mixture in three dimensions. This is typically accomplished using an approximation scheme to evolve a discretized system over a given time at increments of a selected time step. This means that a simulated volume of length X, width Y, and height Z is divided into smaller volumes of dimension $dx \times dy \times dz$, and a value for the phase variable is calculated at time increments of dt for every location in the volume. A common method of approximating solutions to difficult problems, such as the Cahn-Hilliard equation, is the use of a finite difference scheme. Finite-difference formulas utilize Taylor expansions to offer approximations to differential equations with varying degrees of accuracy. Recall the Cahn-Hilliard equation. Numerically solving this equation requires a scheme for the Laplacian operator. To achieve $O(h^2)$ accuracy, we can apply a centered finite difference scheme in three dimensions. A commonly selected form is given by

$$\frac{\partial^2 \phi(x)}{\partial x^2} = \frac{\phi_{i+1} - 2\phi_i + \phi_{i-1}}{dx^2} \tag{4.1}$$

where dx is the spatial step size in their X direction. This can be applied in three dimension by summing the second partial derivatives to suit the dimensionality of your problem. Using this scheme to calculate the chemical potential and its Laplacian, the right side of the equation can be solved for a given time. This provides both the current phase field and the rate at which it is changing, so an approximation at the next time step can be achieved using the Euler method,

$$\phi^{n+1} = \phi^n + dt \frac{\partial \phi^n}{\partial t} \tag{4.2}$$

where dt is the time step and n is the current time. This process is repeated for an amount of simulation time that varies depending on the intentions of the user. However, for certain domains of simulation size, there are more efficient methods that utilize fourier transforms to approximate the solution. These are called spectral methods. Spectral methods generally use fast fourier transforms to decompose a function into a number of sinusoidal elements of various frequencies. This is accomplished by utilizing a series of

algorithms to calculate the discrete fourier transform (DFT) of all available data points. The DFT of a data set is calculated by determining the effect each frequency, or basis function, has in the overall data set through the formula

$$X_k = \sum_{n=0}^{N-1} x_n e^{\frac{-2\pi i k n}{N}} \tag{4.3}$$

where x_n is the sequence of data points, N is the number of data points, k is the frequency of the basis function being considered, and X_k will be the expression telling the weight of that frequency in the overall data set [5]. As opposed to finite difference methods which use a number of surrounding points, this process considers all available data making it a global approximation. In some applications, this allows the use of a coarse mesh while maintaining or improving spatial accuracy. However, when using spectral methods, the size of the data set will often play a factor in the computational efficiency of a simulation. The preferred methods of calculating a DFT in scientific computing are collections of fast fourier transform algorithms (FFT's) [6]. FFT's break a data set down into smaller portions to simplify the calculation of a series of DFT's. One of the most common algorithms used for this divide and conquer strategy is due to Cooley and Tukey [6], which is used when the number of data points is composite, or highly factorable. The basic Cooley-Tukey algorithm is seen below

$$X_k = \sum_{m=0}^{\frac{N}{2}-1} x_{2m} e^{\frac{-2\pi i k (2m)}{N}} + \sum_{m=0}^{\frac{N}{2}-1} x_{2m+1} e^{\frac{-2\pi i k (2m+1)}{N}} \tag{4.4}$$

where $n = 2m$ [6]. The data is being grouped by index into even and odd sets to reduce complexity of the DFT calculation. This can be performed recursively in order to return at most m small sets of points, which reduces the size, and difficulty, of matrix operations in the DFT calculations to increase efficiency. While there are methods for calculating the DFT of prime data sets, such as the prime factor algorithm, it is preferable to choose a size with small factors, making powers of two ideal. This makes simulation size an important consideration when working with large data. Existing FFT packages, such as Fastest Fourier Transforms in the West (FFTW), will utilize the proper algorithm

based on factorization to reduce the computational intensity posed by complicated sizing. This will ensure a high degree of spatial accuracy while time evolution can be handled using a finite difference approximation.

4.3 Model and Analysis

In our experiments, a Cahn-Hilliard-Cook (CHC) model was utilized to study the evolution of immiscible thin-films through surface-directed spinodal decomposition. The CHC equation is given by

$$\frac{\partial \phi}{\partial t} = \nabla \cdot \left(M \nabla \frac{\delta F}{\delta \phi} \right) + \zeta \tag{4.5}$$

where ζ is a randomly generated term which approximates thermal fluctuations in real systems. This variation of the CH equation has been widely used for modeling spinodal decomposition in immiscible systems [7]. The general form of the free energy density was described earlier. However, the bulk term is actually composed of several contributions given by,

$$f = w(f_{pp} + f_{ps}), \tag{4.6}$$

where f_{pp} and f_{ps} represent bulk material and surface attraction forces, respectively, and w is a parameter used to scale the energy curve. The bulk term, which describes the interaction between the two phases, is seen below.

$$f_{pp} = \frac{\phi^4}{4} - \frac{\phi^2}{2} \tag{4.7}$$

The form of f_{pp} is a typical Ginzburg-Landau style double well function with extrema at values of $\phi = \pm 1$. The locations of the energy wells define the two materials in the field, with $\phi = +1$ and $\phi = -1$ representing the wetting and non-wetting phases, respectively. The surface term gives our model the ability to simulate preferential wetting by altering the free energy based on distance from the confining surfaces. f_{ps} is described by

$$f_{ps} = \frac{B(z)(\phi^2 + 2\phi)}{2} \tag{4.8}$$

where the $B(z)$ is a piece-wise, depth dependent function. It was given the form

$$B(z) = \begin{cases} \beta\dfrac{(4-z)\delta}{4}, & 0 < z < 4\delta \\ 0, & 4\delta < z < (n_z - 5)\delta \\ \beta\dfrac{[z-(n_z-5)]\delta}{4} & (n_z-5)\delta < z < n_z\delta \end{cases}, \tag{4.9}$$

where δ is the mesh spacing, z is distance from the lower surface (height), nz is the total thickness of the simulation, and β is a bias used for tuning the wetting strength. With some testing, a bias strength was selected that mimicked the formation of wetting layers seen in previous experiments and simulations [8]. This alteration provided the boundary conditions for the z-dimension while periodic boundaries were applied in x and y to emulate a larger system. Periodic boundaries treat opposite extremes of the space as neighbors, and this is common practice in simulation. The method used to calculate the field variables is a semi-implicit spectral method devised by Zhu and coworkers [9]. Updating the field for a new time step begins with the calculation of the chemical potentials, denoted μ, which simply means evaluating the material derivative of the free energy functional at all locations. The second step requires the calculation of the DFT's of both the concentration field as well as the chemical potentials, which results in

$$\frac{\partial\tilde{\phi}(\boldsymbol{k},t)}{\partial t} = -k^2\frac{\partial\tilde{f_{pp}}}{\partial\phi} - \kappa k^4\tilde{\phi}(\boldsymbol{k},t) \tag{4.10}$$

where a ~represents a transform to fourier space, while $\boldsymbol{k}$ and k are a fourier vector describing the components and its magnitude, respectively [9]. While this could be updated in fourier space using an explicit Euler step, this would have a low degree of accuracy through time. This would require the use of a smaller time step, which could significantly increase the computational resources needed to simulate a given time period. However, a semi-implicit scheme results in significantly higher accuracy in time. By handling the higher order (k^4) term implicitly, you can reach the following equation

$$\tilde{\phi^{t+dt}}(\boldsymbol{k}) = \frac{\tilde{\phi^t}(\boldsymbol{k}) - dtk^2\frac{\partial\tilde{f_{pp}^t}}{\partial\phi}}{1 + dt\kappa k^4} \tag{4.11}$$

where t and $t+dt$ represent the present step and the step to be estimated, respectively [9]. Using this method, we were able to use a significantly larger time step (up to two orders of magnitude larger) while maintaining a high degree of accuracy. In our simulations, a time step of $dt = 0.5$ was used while it is not uncommon for finite difference methods to require step sizes of $dt = 0.001$. This allowed us to use simulate a broad range of system sizes in a comparatively small amount of time. Each of our systems had $nx = ny = 512\delta$ while the thicknesses, nz, ranged from $14 \leq nz \leq 256$. Each simulation coarsened for 100,000 time steps ending at a time of $\tau = 50000$.The mobility, scaling constants and noise terms were all assigned a value of one for simplicity.

In previous works [10], it has been noted that the structure of a thin-film can be altered significantly by varying film thickness. For this reason, we have chosen to explore the potential morphologies that can be obtained as both thickness and composition are decreased into a region that displays similar behavior. This required a method for quantifying different morphologies for easy classification. For this reason, we used a cluster enumeration algorithm to track the evolution of non-wetting material domains. The Hoshen-Kopelman (HK) algorithm is a tool well suited to this purpose [11]. The HK algorithm is a union-find based method that is capable of counting clusters of values that meet a certain criterion using a single pass over that data and a small set of reorganization calculations to provide clarity in the outputs. As each data point is processed, it is compared to previously scanned neighboring points. Each grid location above a provided threshold is assigned a cluster number based on the information that has already been collected. For example, if a data point is surrounded by un-labeled points, it will be considered the first point of a new cluster. However, if one of the relevant neighboring points has a cluster value, the current position would take on the lowest value held by a neighbor. If multiple neighbors hold dissimilar cluster numbers, they are united under the cluster with the lowest value. Figure 4.1 below show a simplified flow of the algorithm.

We applied the HK algorithm to concentration fields produced at selected time steps in each simulation. Being that the pure non-wetting phase is represented by $\phi = 1$, we selected a concentration threshold of $\phi_{min} = 0.2$ to avoid noise caused by small

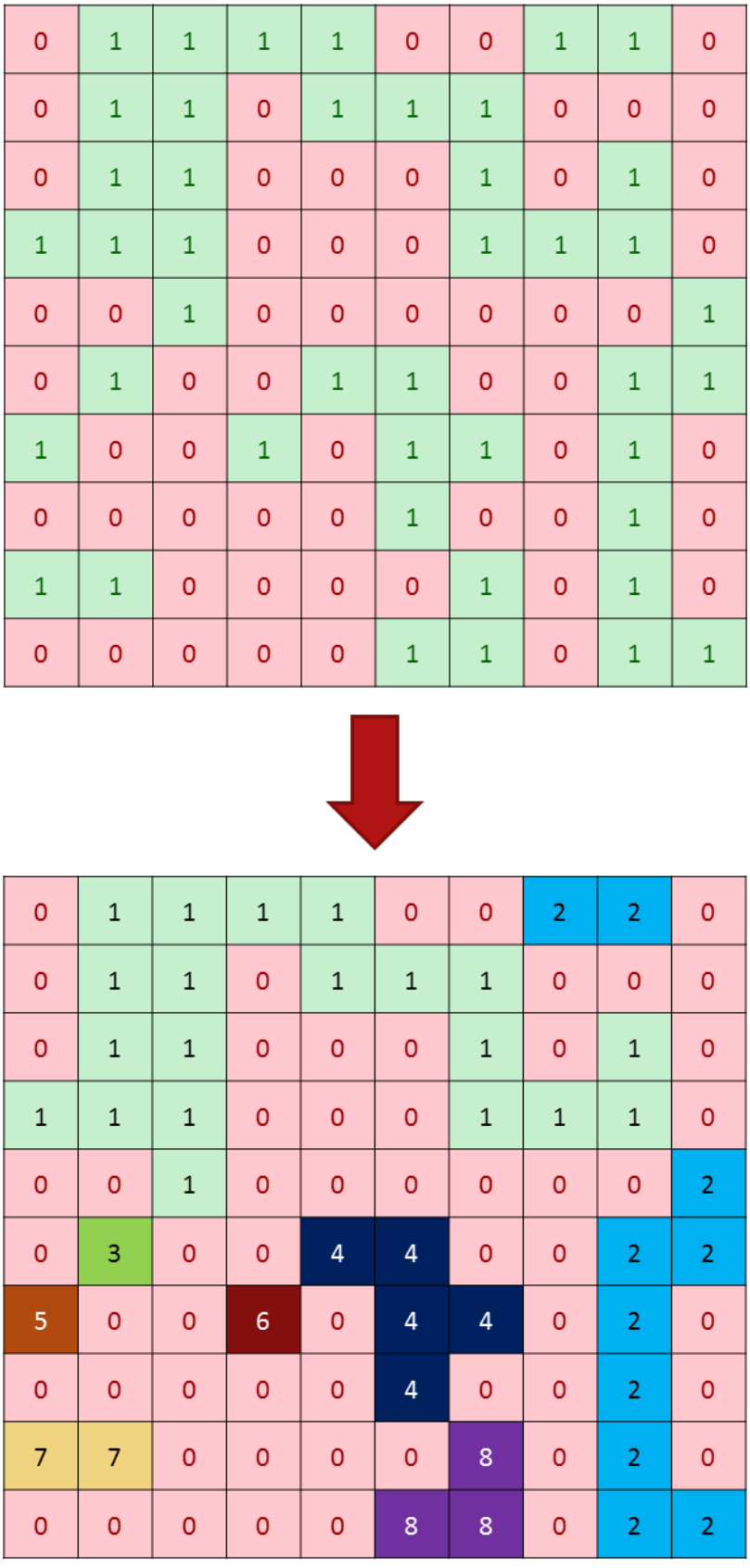

Figure 4.1: Simple case showing result of HK algorithm. Algorithm starts at top left and follows standard raster scan until the entire space has been analyzed.

fluctuations in the interfacial regions. This allowed us to track the simulated volume of every non-wetting domain for each output field. While it does not give morphology directly, this information can be used to calculate the degree of continuity. Continuity has been described in experiments as the weight of non-wetting material remaining after the second phase is chemically etched away divided by the weight of that material used in the mixture [12]. In a similar fashion, we have described continuity as

$$\Gamma_C = \frac{V_L}{V_T}, \tag{4.12}$$

where V_L is the volume of the largest domain of non-wetting material and V_T is the sum of the volumes of all non-wetting domains at that time. An example of the simulation results after analysis by the HK algorithm can be seen in figure 4.2, where each domain has been classified and given a separate label and corresponding color.

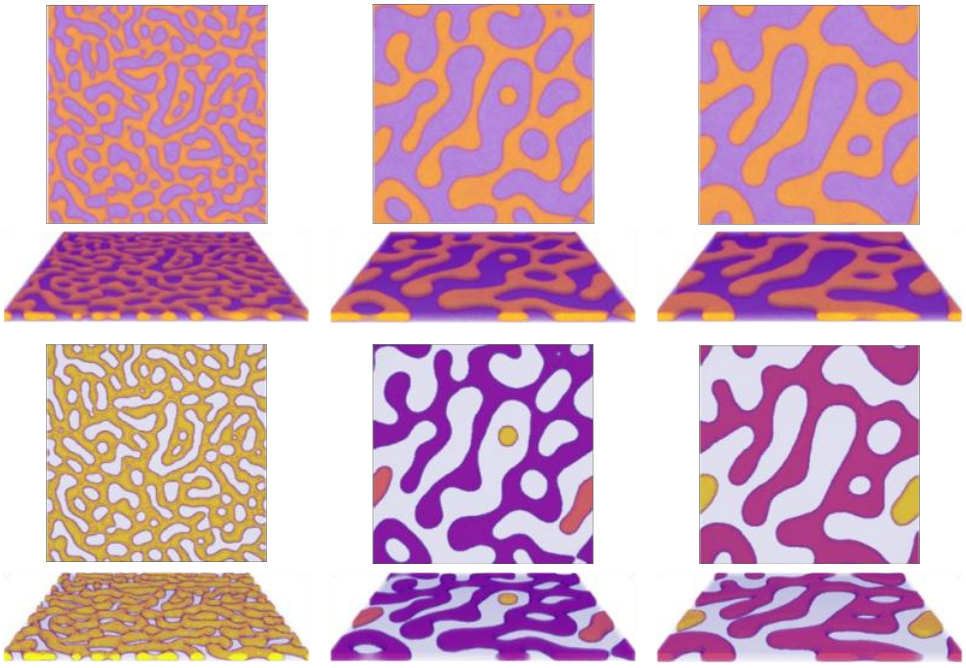

Figure 4.2: Simulation developing into 2D bicontinuous morphology (top) and HK representation (bottom). Images shown are at $\tau = 2500, 25000, 50000$.

Using this parameter, we were able to determine the morphological regions as we moved through the parameter space of film thickness and composition. A rough cut-off for continuity was set at $\Gamma_C = 0.8$. To obtain a statistically valid classification, our primary region of thicknesses and compositions was averaged over twenty runs with initial states

that randomly vary about the same mean value. This data showed some regions with clearly defined morphologies, while others represent a transition in separation kinetics that will be discussed in the following section.

To ensure the accuracy of our model, results at high thicknesses were compared to an experimental work using a PMMA/SAN blend to achieve similar structures. Using this thin-film study [13], early and intermediate stage morphologies were found to be qualitatively similar to real structures for blends with $\phi_{NW} = 0.3$ if a spacing of $\delta = 10$nm was used. Given this length scale and an experimentally obtained diffusion constant of $D = 1.6 \times 10^{-13} \frac{cm^2}{s}$ [14], a simulation time scale of $\tau = 6.25$s was obtained. This gives us a simulation size of 5.12nm $\times$ 5.12nm with varying thickness, and a final time of nearly 87hrs.

Bibliography

[1] John W. Cahn. Phase separation by spinodal decomposition in isotropic systems. *The Journal of Chemical Physics*, 42(1):93–99, 1965.

[2] Subir K. Das, Sanjay Puri, Jurgen Horbach, and K. Binder. Kinetics of phase separation in thin films: Simulations for the diffusive case. *Physical Review E*, 72 (6), 2005.

[3] Lennon O Naraigh and Jean-Luc Thiffeault. Dynamical effects and phase separation in cooled binary fluid films. *Physical Review E*, 76(3), 2007.

[4] Mohammad Tabatabaieyazdi, Philip K Chan, and Jiangning Wu. A computational study of multiple surface-directed phase separation in polymer blends under a temperature gradient. *Modelling and Simulation in Materials Science and Engineering*, 23(7):075004, 2015.

[5] Eric W Weisstein. Discrete fourier transform.

[6] Vladimir Stojanovic. Fast fourier transform: Theory and algorithms.

[7] J. Marro and J.l. Valles. Relevance of the cahn-hilliard-cook theory at early times in spinodal decomposition. *Physics Letters A*, 95(8):443–446, 1983.

[8] Michael J. A. Hore and Mohamed Laradji. Dissipative particle dynamics simulation of the interplay between spinodal decomposition and wetting in thin film binary fluids. *The Journal of Chemical Physics*, 132(2):024908, 2010.

[9] Jingzhi Zhu, Long-Qing Chen, Jie Shen, and Veena Tikare. Coarsening kinetics from a variable-mobility cahn-hilliard equation: Application of a semi-implicit fourier spectral method. *Physical Review E*, 60(4):3564–3572, Jan 1999.

[10] L. Sung, A. Karim, J. F. Douglas, and C. C. Han. Dimensional crossover in the phase separation kinetics of thin polymer blend films. *Physical Review Letters*, 76 (23):4368–4371, Mar 1996.

[11] S. Frijters, T. Kruger, and J. Harting. Parallelised hoshen–kopelman algorithm for lattice-boltzmann simulations. *Computer Physics Communications*, 189:92–98, 2015.

[12] Sandrine Chaput, Christian Carrot, Mickael Castro, and Frederic Prochazka. Co-continuity interval in immiscible polymer blends by dynamic mechanical spectroscopy in the molten and solid state. *Rheologica Acta*, 43(5):417–426, 2004.

[13] Hyun-Joong Chung and Russell J. Composto. Breakdown of dynamic scaling in thin film binary liquids undergoing phase separation. *Physical Review Letters*, 92(18), Jun 2004.

[14] Hua Qiu and Mosto Bousmina. Determination of mutual diffusion coefficients at nonsymmetric polymer/polymer interfaces from rheometry. *Macromolecules*, 33(17): 6588–6594, 2000.

Chapter 5

Results

5.1 Introduction

In experimental studies of SDSD, significant changes in separation kinetics have been attributed to variations in film thickness. However, in many systems it is difficult to gain a full understanding of the process due to the length and time scales on which they occur. For this reason, we have designed a parametric study using our model to study the interplay between bulk separation and preferential wetting of the confining surfaces. By varying film thickness over a small range of blend compositions, we were able to note distinct regions where the formation of wetting layers caused a morphological crossover. Initial exploration provided three morphology classifications that could be achieved in our parameter space: discrete, bicontinuous, and two-dimensionally (2D) bicontinuous. Each combination of film thickness and blend composition was classified by tracking the continuity of the non-wetting phase throughout each simulation. This parameter provided a narrow region that was further probed to determine the limits of the dimensional crossover. Exploration was continued into the space of higher thicknesses and concentrations, and initial classifications for this region were made by extrapolating between conveniently spaced data points. An overview of the explored space will be provided, and examples of the structures obtained will be compared to show the significant effects that preferential wetting can have throughout a film. A plot showing the morphologies of each parametric region will be presented, along with the most likely structures in nearby space. To conclude the chapter, our results will be compared to relevant experiments from literature to for further explanation of the phase separation kinetics in films of similar thicknesses.

5.2 Exploration: Preferential Wetting vs. Bulk Separation

While it is well documented that surface effects can alter the morphology of a system [1–3], their interplay with separation in the bulk is complex. Several works have studied this interplay over a wide range of thicknesses [3, 4]. While these provided valuable

information, they do not give much discussion of the morphologies that can be achieved as a result of preferential wetting. Given the segregated nature of immiscible thin-film blends, it would be sensible to assume that the bulk kinetics will change as a result of the altered composition in the central region. This prompted initial testing to determine what structures are attainable in very thin-films with symmetric surface wetting. We began our study by simulating relatively thin ($nz = 20$ or roughly 200nm) systems with large variations in composition. Using blends with $0.2 \geq \phi_{NW} \geq 0.325$ at increments of $\Delta\phi_{NW} = 0.025$, three clear morphologies (seen in figure 5.1) were recognized.

Figure 5.1: Simulation results displaying the three morphologies of interest: discrete (left), 2D bicontinuous (middle), and bicontinuous or porous (right). Images shown are at $\tau = 2500$ for $nz = 20$ with $\phi_{NW} = 0.2, 0.275, 0.325$ (listed left to right).

At the lower values of ϕ_{NW}, the initial bicontinuous structure typical of spinodal decomposition quickly broke down into a large number of small domains. In this discrete morphology, droplets coalesced to minimize the interface between materials and likely would have continued to form larger domains if they had been allowed to continue coarsening. As ϕ_{NW} was increased, the initial spinodal structure remained intact for extended times. Domains became irregular and their average size increased. This trend continued into a second region, where continuity of the non-wetting phase is maintained. The network of non-wetting material takes on a flattened state, as can be seen in figure 5.2 below.

This is a subset of bicontinuous structures which we will call 2D bicontinuous. This name comes from the high continuity of both phases in the central plane. Out of our initial simulations, only those at $\phi_{NW} = 0.275$ showed this structure. At higher non-wetting

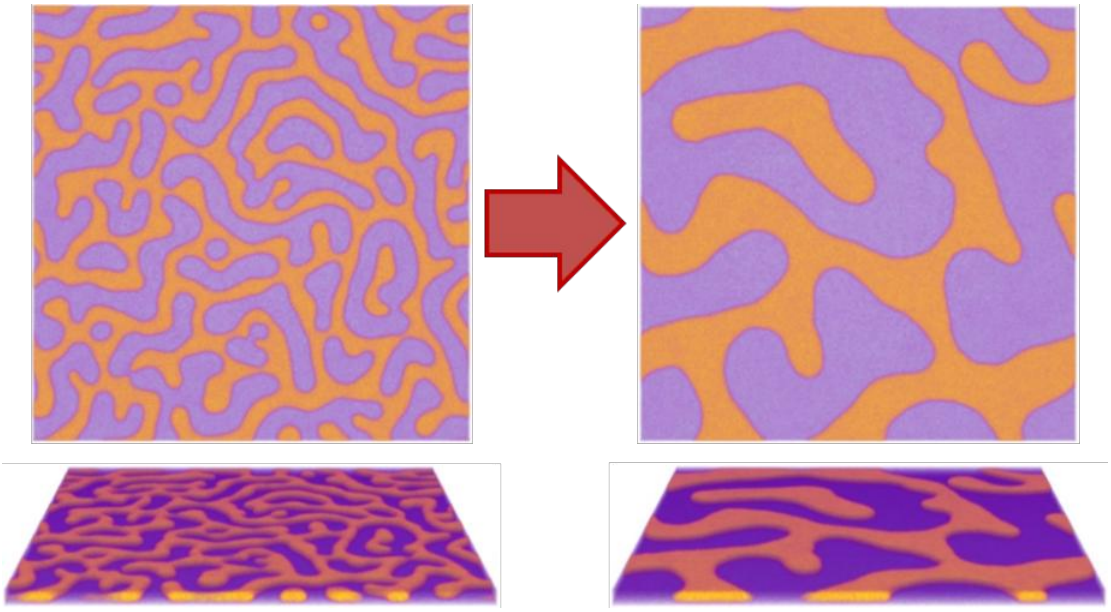

Figure 5.2: Images showing the effects of restricting film thickness on development of a 2D bicontinuous.

concentrations, a second type of bicontinuous structure is seen. While this type would generally have total continuity in non-wetting phase, the central plane is not bicontinuous as seen in figure 5.1. As ϕ_{NW} increases, the pores in the non-wetting layer decrease in size as it tends towards becoming a dense sheet.

Moving forward, we explored how preferential wetting affects films of varying thicknesses for a subset of the previous concentration range. To make the best use of the DFT algorithms while covering a large range of sizes, we selected thicknesses as powers of $nz = 2^n$ where $n = 5, 6, 7, 8$.

At the highest thickness, there is little variation in domain size throughout the thickness of the film. The effects of surface wetting are minimal and the non-wetting phase is characterized by a series of irregularly shaped droplets. This is the result of a lack of interplay between the depleted regions adjacent to the wetting layers. Once a film is sufficiently thin, the composition wave initiated by the formation of the layers can actually be felt throughout the bulk of the film. This is obviously not the case for films that are deep compared to the thickness of said layers. Take figure 5.3 as an example. It is quite clear that compositional change due to segregation near the confining surfaces was insignificant throughout the majority of the film when $nz = 2^8$. This translates to a lo-

calized increase in the density of non-wetting material and slightly altered domain growth near the surfaces. The difference is much more pronounced in a film of significantly lower thickness ($nz = 2^4$), where a suppressed 2d bicontinuous structure is formed.

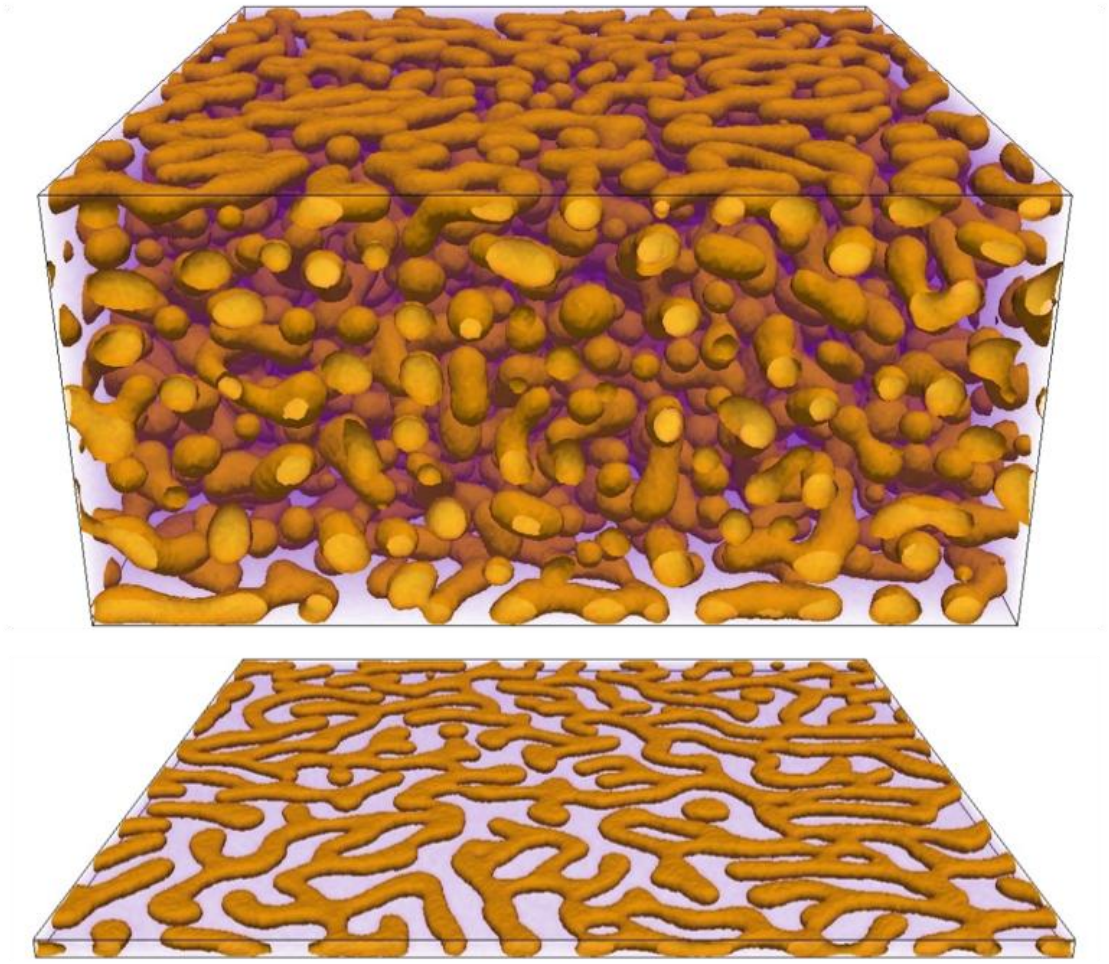

Figure 5.3: Samples showing morphology for $nz = 256, 16$ (top to bottom) at $\phi_{NW} = 0.2625$ at a time of $\tau = 7500$.

However, as thickness decreases for the same concentration, a notable difference can be seen at different depths. For $nz = 2^7$, some hint of the wetting effects can seen as the oddly shaped domains adjacent to the wetting layers grow at an increased rate. Near the confining surfaces, domain shapes are reminiscent of a broken spinodal structure growing at a slightly accelerated rate. With increasing distance from the surfaces, domain size tends to decrease and take on typical droplet shapes. The change in behavior can be seen in figure 5.4.

This pattern continues downwards through $nz = 2^6$ where we begin to see a clear shift due to the compression imposed by the film thickness, as shown below. Near this film

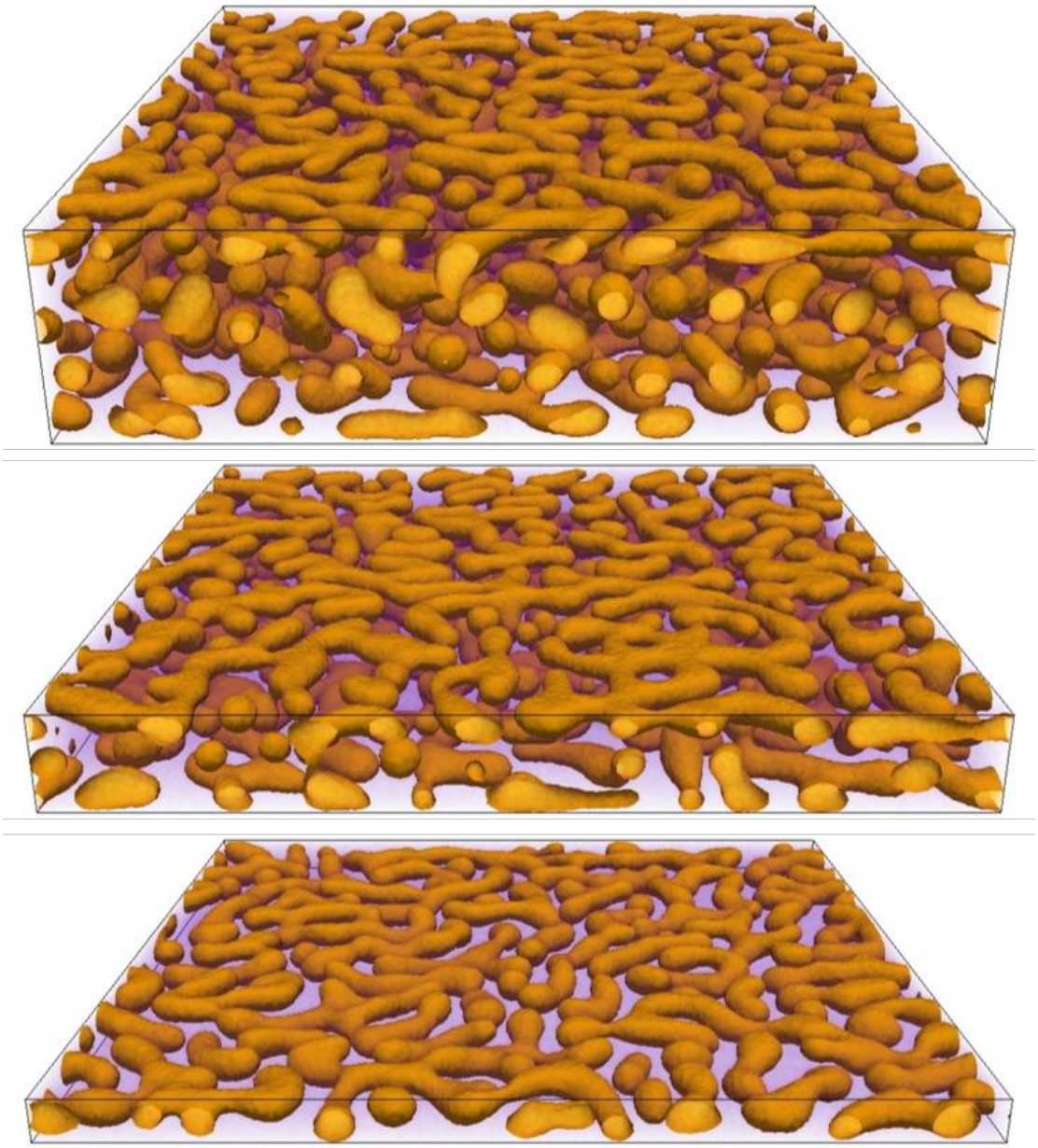

Figure 5.4: Samples showing morphology for $nz = 128, 64, 32$ (top to bottom) at $\phi_{NW} = 0.2625$ at a time of $\tau = 7500$ steps.

thickness, the depletion regions adjacent to the wetting layers begin to intersect. This results in a structure that more closely resembles the two dimensional networks of non-wetting material seen in figure 5.2. However, several simulations at $nz = 2^6$ have shown that an atypical layered structure remains dominant for low ϕ_{NW}. As thickness is continually decreased ($nz < 2^5$), the symmetrical wetting causes an even greater shift in the composition of the central region. To find the extent of these effects at low thicknesses, our primary test space was centered around the location where we discovered the 2D

bicontinuous network. This provided a region of thicknesses $nz = 14, 16, 18, 20, 22, 24, 26$ and compositions $\phi_{NW} = 0.25, 0.2625, 0.275, 0.2875, 0.3$. For every combination of thickness and composition in that region, we averaged the results of twenty simulations to determine its range of possible continuities. Using this as a guideline, we were able to classify setups as likely to produce one of the three previously described morphologies.

5.3 Initial Morphology Classification

Beginning with our lowest concentrations, we saw the formation of small domains as expected. At $\phi_{nw} = 0.25$, all film thicknesses were determined to produce a discrete morphology. The smallest domain sizes were seen at $nz = 26$ where the concentration of wetting material in the middle layer is slightly higher. As film thickness decreases, we saw the potential domain size grow, despite large variations as seen in figure 5.5 below. This was to be expected, as the interaction of the depletion regions should be the most pronounced at our lowest values of nz. This trend can be seen in the plots and corresponding images below.

However, it seemed obvious that a shift was likely to occur as ϕ_{NW} approached the values at which we initially observed the 2D bicontinuous morphology. The next composition, $\phi_{NW} = 0.2625$, was found to be the lower end of the transitional region leading to bicontinuity. The three lowest film thicknesses tested ($nz = 14, 16, 18$) yielded mostly bicontinuous morphologies, while larger films were more likely to experience a breakdown into smaller domains. A similar case was observed for $\phi_{NW} = 0.275$, with an interesting difference. As nz was increased at this composition, we witnessed a shift from a porous layer, to a 2D bicontinuous morphology, to the formation of discrete droplets all within our initial range of thicknesses. This transition can be seen in the representative images of figure 5.6 below.

For higher values of ϕ_{NW}, the trend established by the previous compositions continued. As expected, an increased density of non-wetting material led to both porous and 2D bicontinuous structures. The latter only occurred at higher values of nz where the increased height of the shared depletion region resulted in a composition that was less biased towards the non-wetting phase. The variations in morphology seen at our

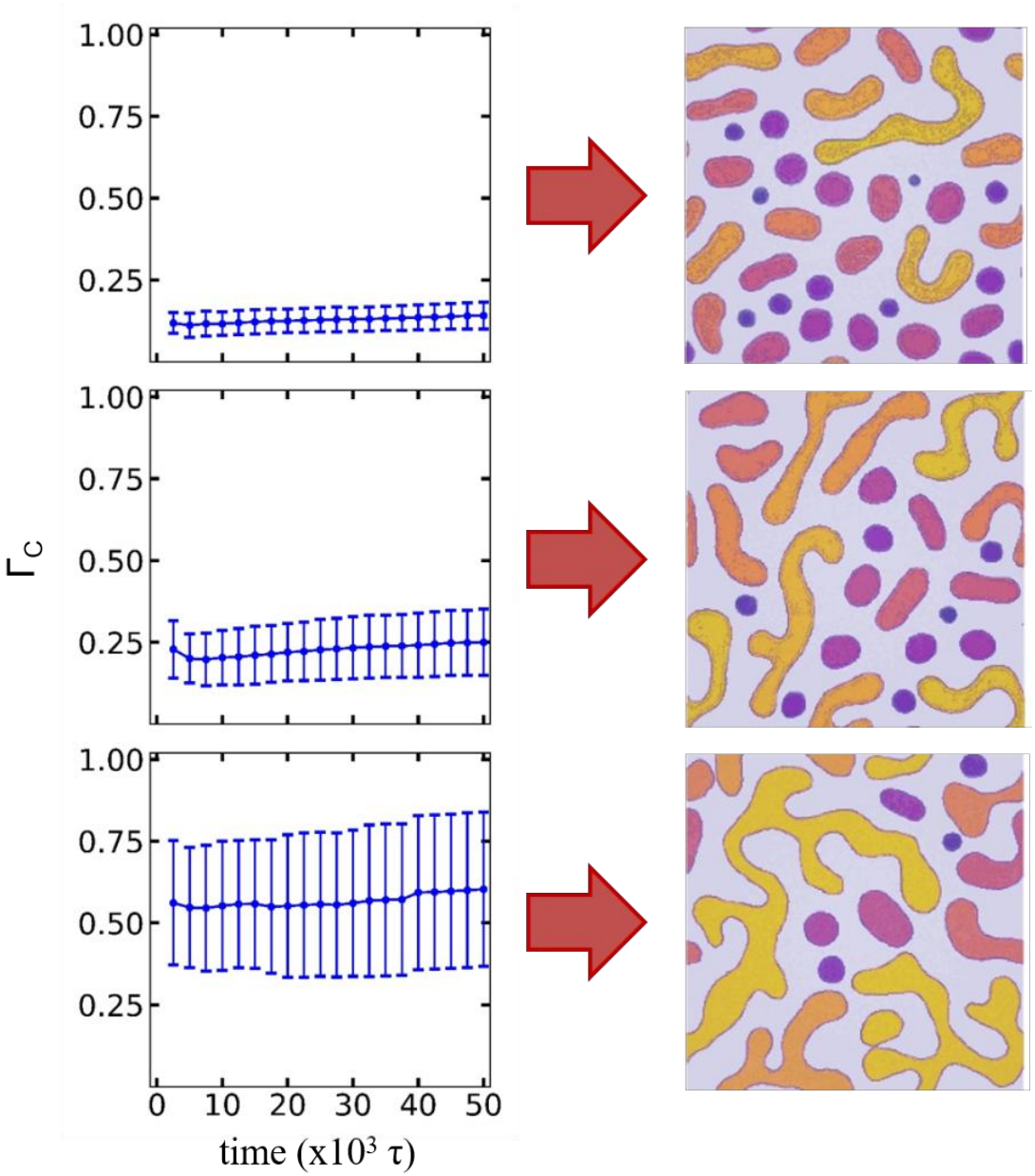

Figure 5.5: Plots showing average continuity factor for $\phi_{NW} = 0.25$ at $nz = 14, 20, 26$ (bottom to top) alongside images displaying the average continuity at that location.

highest initial value of ϕ_{NW} can be seen in figure 5.7 below. The deviation and average Γ_C for simulations at $\phi_{NW} = 0.3$ for low thicknesses had little variation from complete continuity of the non-wetting phase.

It was noted that a portion of the discrete and 2D bicontinuous regions had large variations in continuity. This is generally caused by variations in capillary widths caused by random initializations. If the diameter of a connecting tube drops significantly below the characteristic length scale of non-wetting domains in the system, it is likely to be

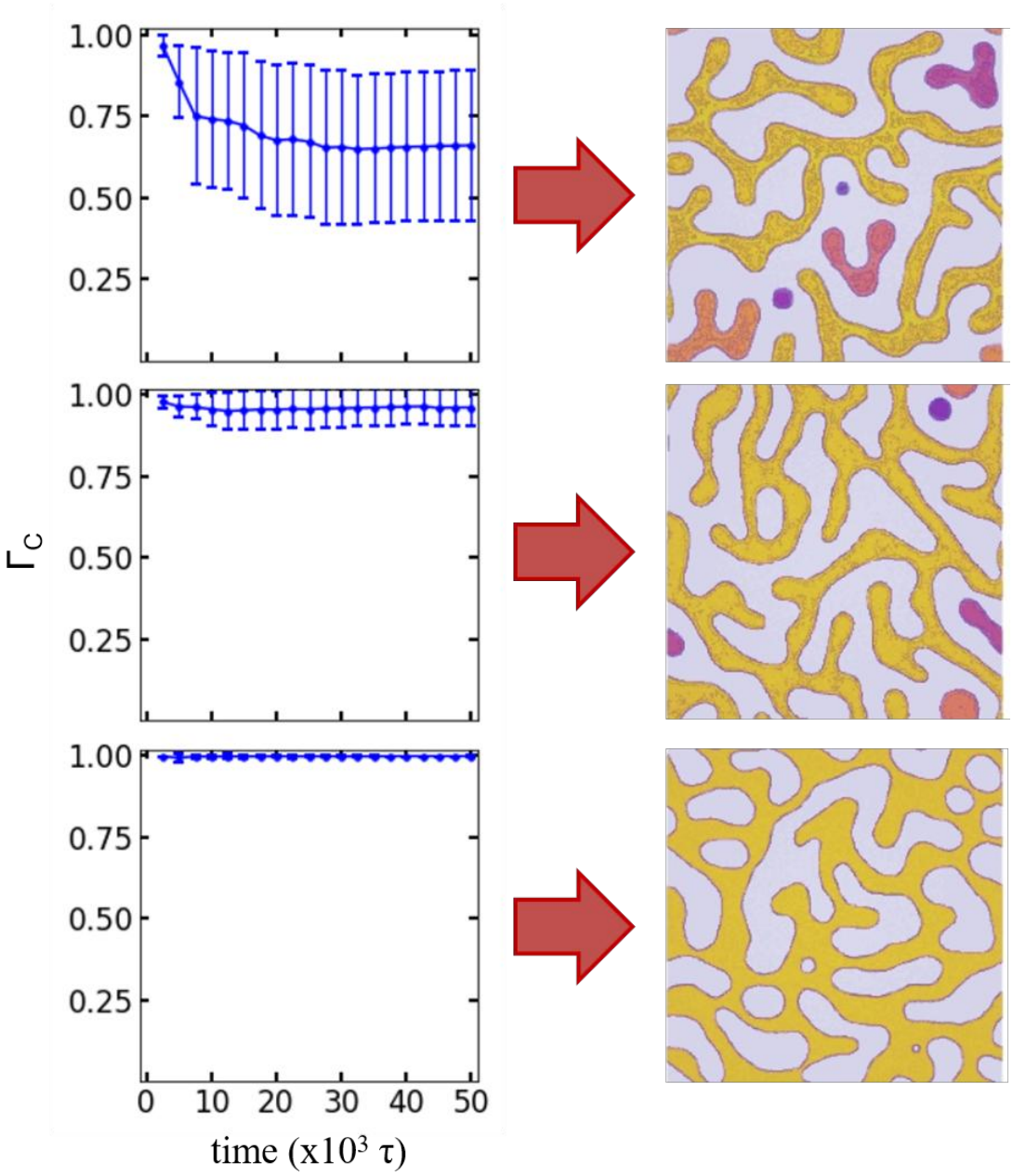

Figure 5.6: Plots showing average continuity factor for $\phi_{NW} = 0.275$ at $nz = 14, 20, 26$ (bottom to top) alongside images displaying the average continuity at that location..

absorbed into the structures that it connects. Since our parameter is akin to a degree of connectivity, the separation of two sizable domains can cause large variations in Γ_C and thus increase the standard deviation. This can be explained through a concept called the percolation threshold. This is a critical system value near which the connectivity of a system changes significantly with minimal difference in the independent variables. This percolation threshold is generally represented through system properties that indicate

high continuity in a material, such as thermal or electrical conductivity in composites [5]. However, this critical value has a significant effect in all percolation problems, including the one presented here. The combinations of film thickness and composition that result in a shift from discrete to 2D bicontinuous structures are close enough to this threshold that thermal noise and random initialization can cause significant changes in the percolation of the system.

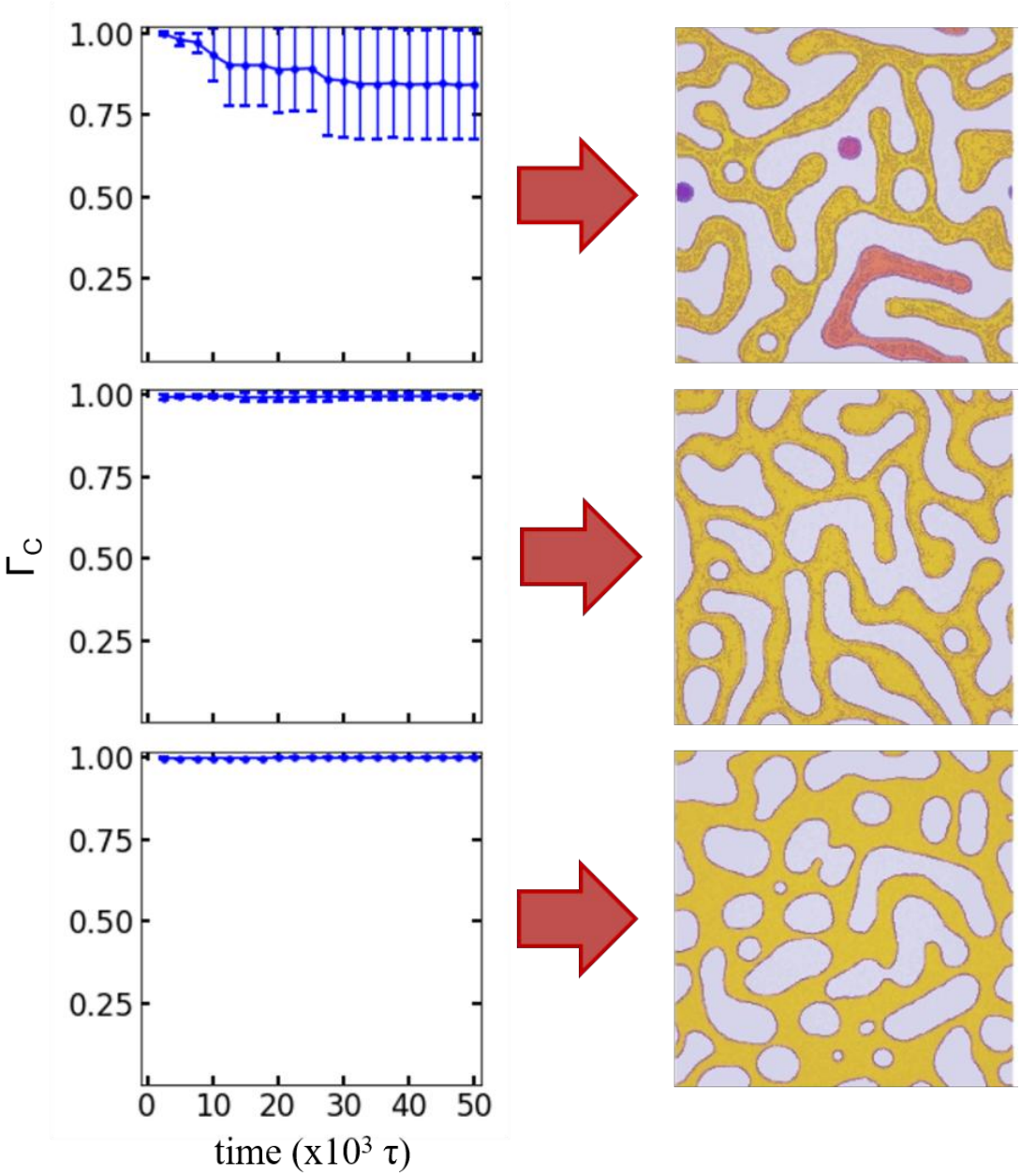

Figure 5.7: Plots showing average continuity factor for $\phi_{NW} = 0.2875$ at $nz = 14, 20, 26$ (bottom to top) alongside images displaying the average continuity at that location.

5.4 Extended Classifcation

Given the rather well-defined morphological regions from our initial study, we continued exploration to see if even larger films were able to maintain a bicontinuous structure. To expand our parameter space, we included $nz = 32, 64$ and doubled the concentration range, which now ends with $\phi_{NW} = 0.35$. To improve our extrapolation, we elected to include simulations with $nz = 40, 50$ for all compositions that were not clearly defined to be in one area. The results from this followed the trends established in the initial parameter space. However, nearly bicontinuous structures at higher thicknesses may only appear to be such due to the need for longer simulations to coarsen. For example, consider the results given by figure 5.8.

Given the near total continuity of the non-wetting phase at $nz = 64$, it would be tempting to classify the regions below it as either 2D or standard bicontinuous. However, examining results for a lower thickness paints a different picture. Given the discrete nature of the sample provided for $nz = 40$, it might be necessary to re-evaluate the previous point. Upon closer inspection, while these morphologies are nearly continuous, these structures will probably be short lived. A combination of viewing angles gives a clearer picture of the tubes connecting larger domains. Another example can be found at the end of our concentration range, $\phi_{NW} = 0.35$, in figure 5.9.

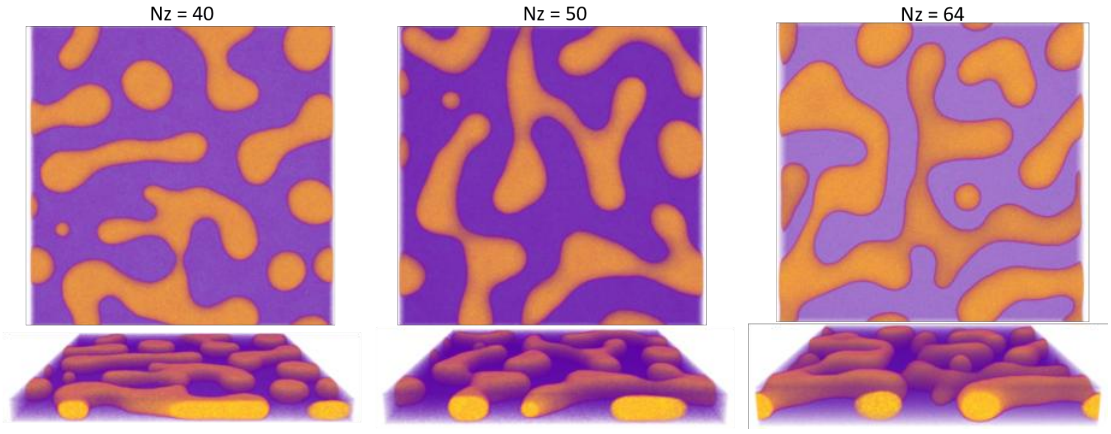

Figure 5.8: Simulation results showing sample morphology for $\phi_{NW} = 0.3$ at $nz = 40, 50, 64$ (left to right).

In figure 5.9, it is quite clear that the lower end of this thickness range produced a film that will remain bicontinuous. Given the amount of non-wetting material forced between

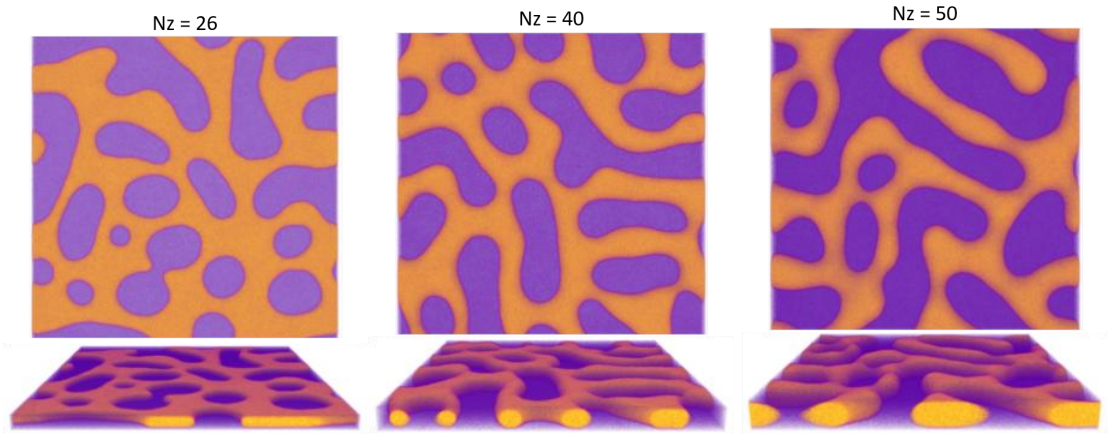

Figure 5.9: Simulation results showing sample morphology for $\phi_{NW} = 0.35$ at $nz = 26, 40, 50$ (left to right).

the wetting layers, this is not surprising. This morphology is actually maintained through $nz = 40$, as can be seen. However, the same cannot be said for our higher thicknesses. While figure 5.9 may seem to be three bicontinuous films at first glance, an angled view of the largest film reveals necking in several of the capillaries. This indicates that the connection will be broken as the tubes are absorbed into larger domain, resulting in a 2D bicontinuous structure. By analyzing all results obtained over our larger parameter space, we were able to confidently define larger morphological regions, as can be seen in figure 5.10.

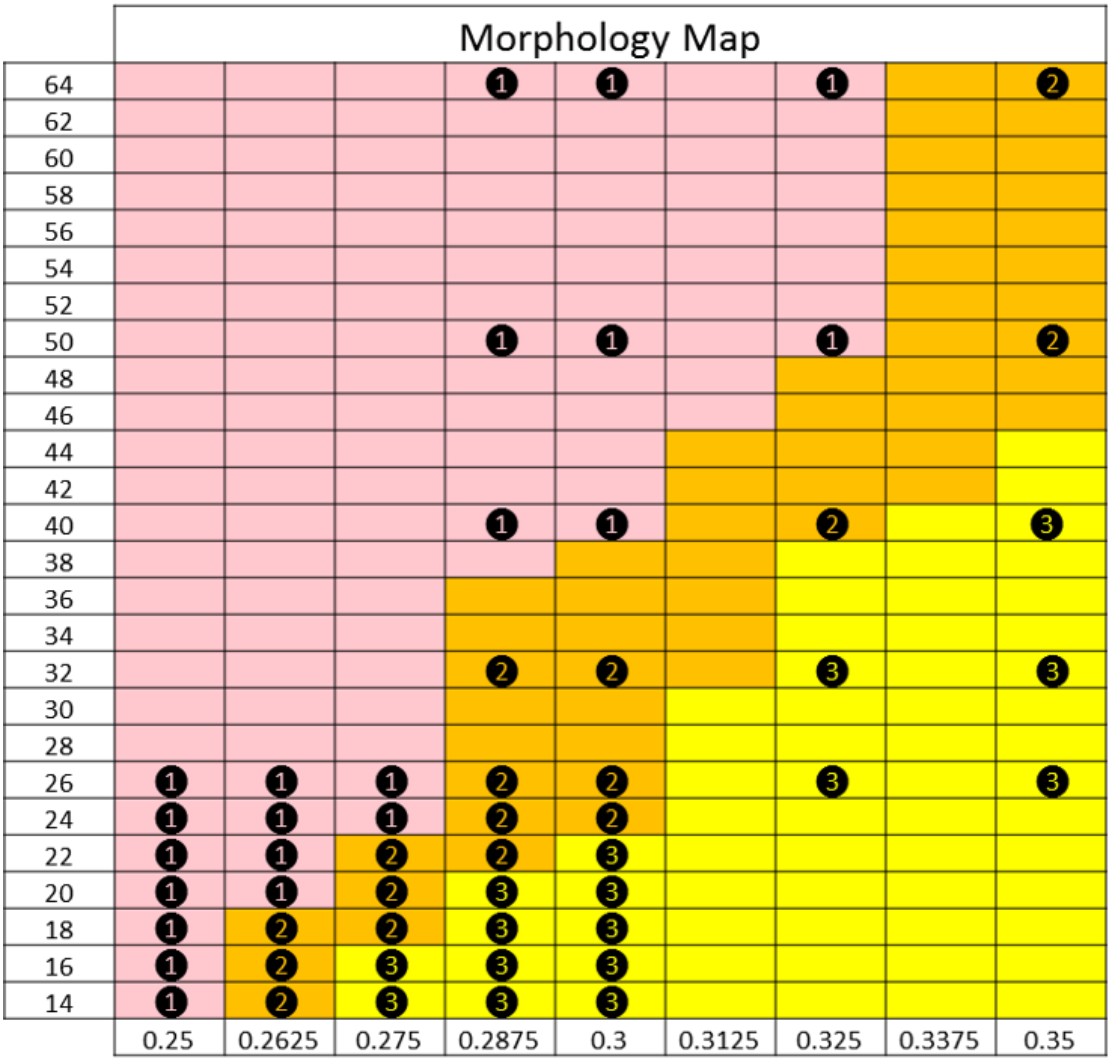

Figure 5.10: Suggested morphology map showing likely structure for values of nz (vertical) at each value of ϕ_{NW} (horizontal). One, two and three along with their associated colors represent discrete, 2D bicontinuous, and bicontinuous structures, respectively.

Bibliography

[1] Richard A. L. Jones, Laura J. Norton, Edward J. Kramer, Frank S. Bates, and Pierre Wiltzius. Surface-directed spinodal decomposition. *Physical Review Letters*, 66(23): 3087–3087, Oct 1991.

[2] M. Geoghegan, R. A. L. Jones, and A. S. Clough. Surface directed spinodal decomposition in a partially miscible polymer blend. *The Journal of Chemical Physics*, 103 (7):2719–2724, 1995.

[3] Howard Wang and Russell J. Composto. Thin film polymer blends undergoing phase separation and wetting: Identification of early, intermediate, and late stages. *The Journal of Chemical Physics*, 113(22):10386–10397, Aug 2000.

[4] L. Sung, A. Karim, J. F. Douglas, and C. C. Han. Dimensional crossover in the phase separation kinetics of thin polymer blend films. *Physical Review Letters*, 76 (23):4368–4371, Mar 1996.

[5] Fuan He, Sienting Lau, Helen Laiwa Chan, and Jintu Fan. High dielectric permittivity and low percolation threshold in nanocomposites based on poly(vinylidene fluoride) and exfoliated graphite nanoplates. *Advanced Materials*, 21(6):710–715, Feb 2009.

Chapter 6

Conclusions

Thin-film materials are already being utilized in many industries, and that number is only going to increase as the push for new technology drives us forward. This makes a full understanding of the processes through which they are produced crucial as we seek newer and better solutions to modern problems. Given their application in all realms, from medicine to consumer electronics, all knowledge of the mechanics through which they form is valuable. This work studied what is possible when something as simple as preferential surface wetting acts on a phase separating blend. As has been seen before [1–4], the interplay between the surface effects and bulk phase separation can yield results that would have been otherwise difficult to obtain. The 2D bicontinuous morphology that was described in previous sections came about because of symmetric wetting. This adds another important factor to consider, as the altered growth near the wetting layers in symmetric systems can compound if films are below a certain thickness. Taking advantage of the overlap that occurs with complete wetting on both sides resulted in a continuous non-wetting phase at low concentrations. Using only small variations in composition or thickness, we were able to obtain significant changes in film structure, with some shifting from discrete domains to a traditional bicontinuous form over a region which yields a 2D bicontinuous morphology. With further research into this region, symmetric surface wetting could be used to gain fine control over the flux through a thin-film, or possibly even a real porosity for filtration membranes. This could be useful in the design of various composite films.

Moving forward, it would be useful to analyze these films as a function of composition to gain deeper understanding of the events that occur under symmetric wetting conditions. This would provide a more accurate explanation of the changes seen as film thickness was varied. It would also be necessary to study various arrangements by further altering the free energy. While this study focuses on the case where the two confining surfaces exert the same attractive force, this is often not the case. Arrangements using

two different confining surfaces would be equally simple to implement and could yield vastly different structures than those explained here.

Bibliography

[1] Hajime Tanaka. Wetting dynamics in a confined symmetric binary mixture undergoing phase separation. *Physical Review Letters*, 70(18):2770–2773, Mar 1993.

[2] L. Sung, A. Karim, J. F. Douglas, and C. C. Han. Dimensional crossover in the phase separation kinetics of thin polymer blend films. *Physical Review Letters*, 76 (23):4368–4371, Mar 1996.

[3] Howard Wang and Russell J. Composto. Thin film polymer blends undergoing phase separation and wetting: Identification of early, intermediate, and late stages. *The Journal of Chemical Physics*, 113(22):10386–10397, Aug 2000.

[4] Hyun-Joong Chung and Russell J. Composto. Breakdown of dynamic scaling in thin film binary liquids undergoing phase separation. *Physical Review Letters*, 92(18), Jun 2004.